

Technical University of Denmark



## Neutron radiography at the Risø National Laboratory

**Domanus, Joseph Czeslaw; Gade-Nielsen, G.; Knudsen, P.; Olsen, J.**

*Publication date:*  
1981

*Document Version*  
Publisher's PDF, also known as Version of record

[Link back to DTU Orbit](#)

*Citation (APA):*  
Domanus, J. C., Gade-Nielsen, G., Knudsen, P., & Olsen, J. (1981). Neutron radiography at the Risø National Laboratory. (Risø-M; No. 2320).

## DTU Library

Technical Information Center of Denmark

---

### General rights

Copyright and moral rights for the publications made accessible in the public portal are retained by the authors and/or other copyright owners and it is a condition of accessing publications that users recognise and abide by the legal requirements associated with these rights.

- Users may download and print one copy of any publication from the public portal for the purpose of private study or research.
- You may not further distribute the material or use it for any profit-making activity or commercial gain
- You may freely distribute the URL identifying the publication in the public portal

If you believe that this document breaches copyright please contact us providing details, and we will remove access to the work immediately and investigate your claim.

RISØ-M-2320

NEUTRON RADIOGRAPHY AT THE RISØ NATIONAL LABORATORY

J.C. Domanus, P. Gade-Nielsen, P. Knudsen, and J. Olsen

Abstract. In this report six papers are collected which will be presented at the First World Conference on Neutron Radiography in San Diego, U.S.A., 7 - 10 December 1981.

They are preceded by a short description of the activities of Risø National Laboratory in the field of post-irradiation examination of nuclear fuel.

One of the nondestructive methods used for this examination is neutron radiography.

In the six conference papers different aspects of neutron radiography performed at Risø are presented.

INIS descriptors: FUEL ELEMENTS; NEUTRON RADIOGRAPHY; POST-IRRADIATION EXAMINATION; RISØE NATIONAL LABORATORY.

November 1981

Risø National Laboratory, DK 4000 Roskilde, Denmark

**ISBN 87-550-0807-0**

**ISSN 0418-6435**

**Risø Repro 1981**

## **CONTENTS**

### **POST IRRADIATION EXAMINATION OF NUCLEAR FUEL AT THE RISØ NATIONAL LABORATORY**

**P. Knudsen**

### **SIX YEARS EXPERIENCE WITH THE DOUBLE BEAM NEUTRON RADIOGRAPHY FACILITY AT THE RISØ NATIONAL LABORATORY**

**P. Knudsen and J. Olsen**

### **DEFECTS REVEALED BY NEUTRON RADIOGRAPHY IN LIGHT WATER REACTOR FUEL**

**J.C. Domanus**

### **SEARCH FOR ADEQUATE QUALITY STANDARDS FOR NEUTRON RADIOGRAPHY OF NUCLEAR FUEL**

**J.C. Domanus**

### **EURATOM TEST PROGRAM FOR IMAGE QUALITY AND ACCURACY OF DIMENSIONS**

**J.C. Domanus**

### **HOW GOOD IS THE NITROCELLULOSE FILM FOR NEUTRON RADIOGRAPHY?**

**J.C. Domanus**

### **MEASURING SIGNAL-TO-NOISE RATIO OF TYPICAL NEUTRON RADIOGRAPHS**

**P. Gade-Nielsen and J. Olsen**

**POST-IRRADIATION EXAMINATION OF NUCLEAR FUEL**  
**AT THE RISØ NATIONAL LABORATORY**

Per Knudsen  
Metallurgy Department  
Risø National Laboratory  
DK-4000 Roskilde  
Denmark

Extensive post-irradiation examinations of water reactor fuels are performed in the hotcells of Risø National Laboratory. These fuels come from Danish development programs [1], from irradiations in foreign power and test reactors [2] and from the internationally sponsored "Risø Fission Gas Project" [3].

Both  $UO_2$  and mixed-oxide fuels, clad in Zircaloy, have been examined at maximum exposures exceeding 50,000 MWD/tU. There has been a range of fuel pins, from 15 cm test fuel pins to 3 m long power reactor fuel pins. The examinations have for instance emphasized cladding performance in failure testing ("ramp tests") or fuel behaviour in steady-state irradiation as well as over-power transients late in life ("bump tests").

A wide variety of non-destructive and destructive examinations (NDE, DE) are used for the evaluation of these fuels. Among the techniques used routinely are:

**NDE**

- visual inspection
- diametral profilometry
- eddy-current testing
- axial gamma scanning
- neutron radiography (NR)

**DE**

- fission gas sampling of fuel pins
- metallography of fuel and cladding
- radial micro gamma scanning
- retained gas measurements
- isotope and burnup analysis.

In this context, NR is used partly as a supplement to the other non-destructive techniques, and partly for the characterization of features which would otherwise require more expensive examination.

This report contains the following six Risø contributions to the World Conference on Neutron Radiography in San Diego (USA), 7-10 December 1981:

1. "Six Years' Experience with the Double Beam Neutron Radiography Facility at the Risø National Laboratory", by P. Knudsen, J. Olsen.
2. "Defects Revealed by Neutron Radiography in Light Water Reactor Fuel", by J. C. Domanus.
3. "Search of Adequate Standards for Neutron Radiography of Nuclear Fuel", by J. C. Domanus.
4. "Euratom Test Program for Image Quality and Accuracy of Dimensions", by J. C. Domanus.

5. "How Good is Nitrocellulose Film for Neutron Radiography?", by J. C. Domanus.

6. "Measuring Signal-to-Noise Ratio of Typical Neutron Radiographs", by P. Gade-Nielsen and J. Olsen.

These papers describe the experience from completed and ongoing fuel examinations as well as several programs for the development of the NR technique.

The first two papers give a description of the Risø NR facility and of a classification of the observations from more than 2000 radiographs. The following two papers explain development programs to improve NR standards for image quality and dimensional measurements; these programs are sponsored by Euratom and managed by Risø. Finally, two papers are included on Risø-sponsored developments: Comparison of nitrocellulose films with the conventional silver halide films, and measurements of signal-to-noise ratio of neutron radiographs.

#### REFERENCES

- [1] Metallurgy Department, Progress Report for the Period 1 January to 31 December 1980, Risø-R-444 (1981).
- [2] See for example:  
BAGGER C., CARLSEN H., DOMANUS J.C., HOUGAARD H., LARSEN E., LARSEN N., Experiment Data Report, IFA 226 Post-Irradiation Examination, TREE-NUREG-1173 (1977).
- [3] KNUDSEN P., Overview of the Risø Fission Gas Project, presented at the DOE/EPRI Contractors' Meeting, Atlanta (USA), 8-9 April 1980.

**SIX YEARS' EXPERIENCE WITH THE DOUBLE BEAM  
NEUTRON RADIOGRAPHY FACILITY AT THE  
RISØ NATIONAL LABORATORY**

P. Knudsen and Jørgen Olsen  
Risø National Laboratory  
DK-4000 Roskilde, Denmark

**ABSTRACT**

The Risø neutron radiography (NR) facility utilizes a homogeneous solution-type reactor (L-55, Atomic International) as the neutron source. Two horizontal, parallel neutron beams, each having a cross section of 10 x 10 cm and a thermal neutron flux of  $10^6$  n/cm<sup>2</sup>·s are available. The collimators are so arranged that the L/D-ratio vertically and horizontally is 110 and 30, respectively.

The principal application of the Risø facility is the nondestructive examination of water reactor fuel, i.e. Zircaloy clad uranium dioxide. This has included 3 m long power reactor fuel rods and 15-200 cm fuel rods from test reactor irradiations. Pin lengths up to 4½ m can be examined. The burnup of some of this fuel exceeds 50,000 MWD/tU.

The NR technique is useful for the characterization of features which would otherwise normally require destructive examination. Examples are: pellet cracks and center voids, local hydriding of the cladding, and presence of water in defect fuel rods. The usefulness of the technique is very much increased by detailed correlation with other methods such as visual inspection, eddy-current testing, axial gamma scanning, and profilometry. Consequently, it is possible to limit the costly destructive examinations, such as metallography, to sample locations of real importance.

The paper presents typical and illustrative examples from the six years of NR experience at Risø.

## INTRODUCTION

The Risø neutron radiography (NR) facility is mainly used for the examination of irradiated water reactor fuel.

The present paper provides a brief description of the facility and details of its application. Typical examples of the experience obtained over six years of operation are given.

### THE RISØ DOUBLE BEAM NEUTRONRADIOGRAPHY FACILITY

The DR 1 (Danish Reactor No. 1) is a homogeneous solution type reactor designed by Atomic International, U.S.A. It provides a maximum thermal neutron flux of  $6 \cdot 10^{10}$  n/cm<sup>2</sup> sec., and a fast neutron flux of  $12 \cdot 10^{10}$  n/cm<sup>2</sup> sec., at the maximum used power level, 2 kW. The spherical core tank has a diameter of 32 cm and is positioned at the centre of a graphite cylinder with a diameter of 152 cm.

The Risø double beam neutron radiography facility is schematically shown on fig 1. Two graphite blocks (3) positioned tangentially to the reactor core (2) have been removed from the reflector (1) thus permitting the neutrons to emerge through the reactor shielding as two beams.

The thermal neutron beam reaching the object to be radiographed has an intensity of  $1.8 \cdot 10^6$  n/cm<sup>2</sup> sec. at the left port, and  $1.4 \cdot 10^6$  n/cm<sup>2</sup> sec. at the right port.

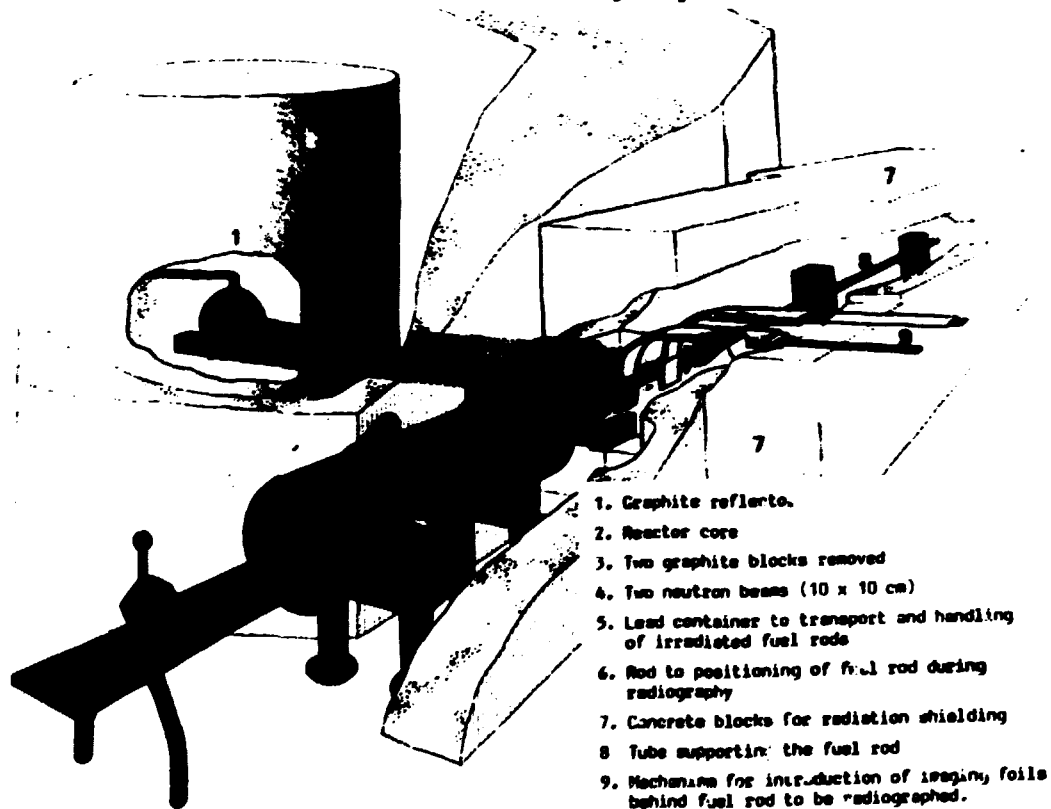


Fig. 1. Double beam neutron radiography facility at Risø



The irradiated nuclear fuel rods are transported from the Hot Cell facility to the DR 1 reactor in a dual-purpose transport/exposure container (5). At the back of this container a steel rod (6) is attached, by the use of which the fuel rod (8) can be pushed out of the container and positioned in the two neutron ports. This part of the rod which has left the shielding container (5), enters a shielded enclosure made of concrete (7). The imaging foils is introduced behind the fuel rod to be radiographed by means of the mechanism (9) consisting of two curved guides, which accommodate the foils and press them towards the rod. The neutron beam, originated at the reactor core (2), is collimated in the graphite collimator, having an inlet of 2 cm (vertically) x 8 cm (horizontally), and an outlet of 10 x 10 cm<sup>2</sup>. The distance between the inlet and exposure surface is 220 cm, which gives an L/D ratio of 110 (in the vertical direction).

The cadmium ratio (measured with 100 mg/cm<sup>2</sup> gold foils) is 4.2 at the left port, and 3.8 at the right port.

#### PROCEDURE

For the purpose of transport of fuel rods between the Hot Cells and the DR 1 reactor two multi-purpose transport/exposure containers are available. One is designed to accommodate fuel rods up to 2.5 m in length and the other up to 4.5 m. The fuel rods to be neutron radiographed are placed in an 1 mm thick aluminium tube in the Hot Cells. This tube protects the container from contamination, and serves at the same time for manipulation of the fuel rod via a steel rod which is fastened to one of its ends. At the end of the steel rod a square or hexagonal plate (6) can be affixed. With the plates rotation of the rod is possible in steps of 90° or 60°, respectively.

A 0.1 mm dysprosium activation transfer foil is used (40 x 120 mm). This foil is introduced through the guiding mechanism (9) to be in close contact with the rod under examination. After the exposure (about 30 min. for Agfa-Gevaert Structurix D4 film or 90 min. for Kodak single coated SR film), the Dy foil is removed from the exposure mechanism (9) and transported to the darkroom. Here X-ray film is placed at both sides of the foil and the foil with the film is inserted into a plastic vacuum cassette. The films are exposed by the Dy foil overnight and are developed the next day.

The fuel rod under examination is exposed through both neutron ports (4 on fig. 1). The first exposure starts when one end of the rod is positioned approximately in the middle of the right port. Simultaneously with the exposure through the right port an exposure through the left port occurs. Due to the difference in the neutron flux intensities the exposure through the left port is a little shorter than through the right port. The rod is moved in steps of 10 cm to cover the entire length.

At the bottom of each neutron port, two cobalt wires are located which serves to provide a positioning index on each film. The developed films are eventually assembled in such a way as to give a single neutron radiograph of the whole rod.

## APPLICATION

The principal application of the Rise NR facility is the non-destructive examination of irradiated water-reactor type fuel, i.e. Zircaloy-clad uranium dioxide or uranium/plutonium dioxide. The examinations have comprised 3 m long power reactor fuel rods as well as 15-200 cm long rods irradiated in test reactors. Rod diameters are in the range 10-15 mm. The irradiation exposure of these fuel rods ranges from 1,000 MWD/tU (a few weeks of irradiation) up to beyond 50,000 MWD/tU (corresponding to several years' exposure).

The components of these fuel rods are illustrated on fig. 2, showing both a standard fuel rod and a special instrumented test fuel rod.

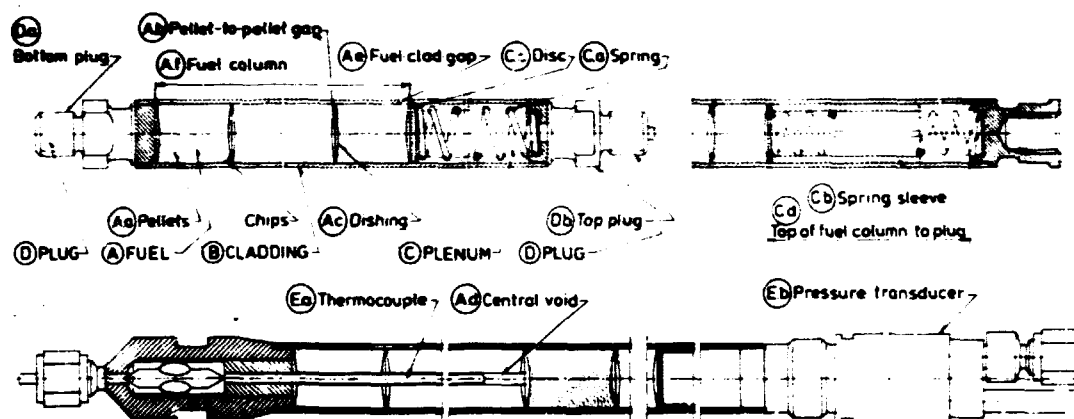


Fig.2. Standard fuel rod (top left), special design of hold-down spring device (top right) and test fuel rod with central thermocouple and fission gas pressure transducer (bottom).

The purpose of NR of irradiated fuel is to check the integrity of and detect/locate defects and dimensional changes in the fuel rod as a whole as well as its individual components. NR is used partly as a supplement to other non-destructive techniques, and partly for the characterization of features which would otherwise require destructive examination.

The usual examination procedure is then:

- (a) use the fast methods of eddy-current testing (ECT), profilometry and axial gamma scanning;
- (b) define the extent of the more time consuming visual inspection and NR;
- (c) from the above examinations determine sample positions for expensive destructive examinations such as for instance metallography, examination of the cladding inside.

## EXPERIENCE

More than 2000 neutron radiographs have been produced during the examination of irradiated fuel at Risø. The various observations have been classified, and typical examples have been assembled in an atlas with film reproductions [1]. Examples of observations are:

### Fuel:

- pellet cracks and chips
- center-void formation
- dish filling

### Cladding:

- Hydriding of the cooler end welds and plenum areas, also of heavily corroded areas of the cladding wall along the fuel column
- localized hydriding of the cladding wall in failed pins, from water ingress.

### Rod:

- Integrity of fuel column, formation of axial gaps, pellet chips in such gaps
- integrity and proper location of plenum spring device and pin instrumentation.

The usefulness of the NR technique is increased by detailed correlation with other non-destructive techniques and two examples shall be mentioned, both with failed rods. In the first case [2], NR indication of local hydriding (verified metallographically) correlated with a large diameter increase on the profilometer trace, fig. 3. This shows that profilometer measurements on failed fuel rods do not only reflect general performance factors such as clad creep-down and ridge formation.

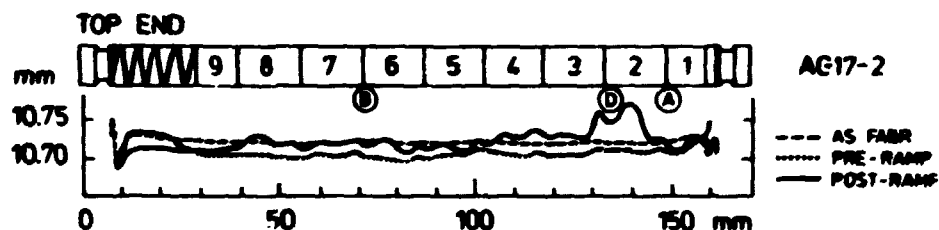


Fig. 3. Large diameter increase near the interface of pellets no. 2 and 3.

In the other case [3], NR was used to evaluate ECT observations. Fig. 4 shows one type of ECT signal at pellet interfaces 5/6 and 6/7 and another signal at interface 2/3; only the latter position had hydride indications in NR. Supporting metallography (pos. II) revealed heavy hydriding here, but no cladding cracks; the other signal type was shown (pos. I) to originate from three large, brittle stress-corrosion type cracks.

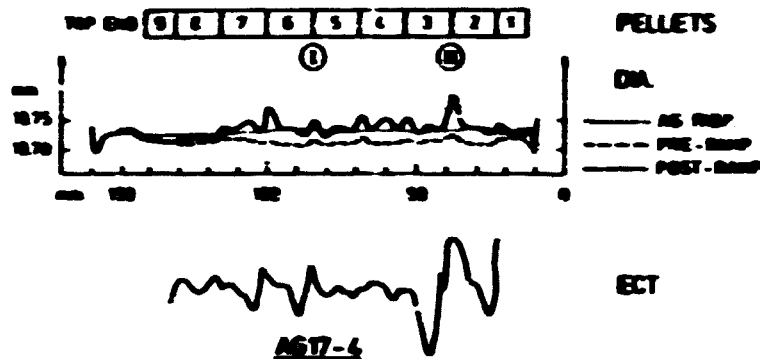


Fig. 4. Eddy-current signals without (I) and with (II) NR indication of hydriding

In a different case, NR gave information as to when the cladding of a fuel rod was defected. This rod had been irradiated for several years in a heavy-water cooled reactor. Upon arrival to the Hot Cells, one end plug was broken off, and NR revealed hydriding (deuteriding?) of the fracture zone. NR also showed the presence of small amounts of a liquid in the plenum. NR exposures of dummy pins with injected traces of  $H_2O$  and  $D_2O$  showed the  $H_2O$  clearly more light-coloured than the  $D_2O$ , due to the difference in neutron cross sections. By comparison it was concluded that the liquid in the broken pin was  $D_2O$ . The cladding must, therefore, have defected already during the irradiation although it cannot be excluded that the final breakage occurred in handling or transport after termination of the irradiation.

#### Recommendations for future work

In the future we intend to use digitizing equipment to analyze the neutron radiographs [5]. With such an equipment it will be possible to make an image processing and in a routine way to give a lot of data about the fuel.

#### REFERENCES

- [1] DOMANUS, J.C., Neutron Radiographic Findings in Light Water Reactor Fuel, Risø National Laboratory, Roskilde (1979).
- [2] KNUDSEN, P., BAGGER, C., FISHLER, M., Characterization of Power Ramp Tests, Proc. ANS Topical Meeting on Water Reactor Fuel Performance, St. Charles (Ill.), pp. 243-252 (1977).
- [3] KNUDSEN, P., BAGGER, C., CARLSEN, H., PWR Type Overpower Tests at 1620 GJ/kgU (18,800 MWD/MTU), Proc. ANS Topical Meeting on Light Water Reactor Fuel Performance, Portland, Ore.), pp. 264-274 (1979).
- [4] GADE-NIELSEN, P., OLSEN, J., Measuring Signal-to-Noise Ratio of Typical Neutron Radiographs, The first world conference on Neutron Radiography, San Diego (1981).

DEFECTS REVEALED BY NEUTRON RADIOGRAPHY  
IN LIGHT WATER REACTOR FUEL

J.C. Domanus

Nuclear Department  
Elsinore Shipbuilding & Engineering Co. Ltd.\*)  
DK-3000 Helsingør, Denmark

ABSTRACT

From neutron radiographs made routinely at Risø National Laboratory for the quality and performance control of nuclear fuel, radiographs showing typical defects in nuclear fuel were chosen.

The defects were classified according to their location, nature and origin.

A collection of reference neutron radiographs was published as an atlas: "Neutron radiographic findings in light water reactor fuel", in which 36 neutron radiographs are produced on film (in original size) and on paper (twice enlarged).

It is intended to enlarge the collection with further examples of defects occurring in nuclear fuel.

---

\*) Work performed under contract with Risø National Laboratory.

## PREFACE

As a contribution to the Neutron Radiography Working Group program, Risø National Laboratory has compiled an atlas of reference neutron radiographs\*). This atlas was published on behalf of Euratom in June 1979 and was distributed to all NRWG members. It contains a collection of defects revealed by neutron radiography in light water reactor fuel, which are reproduced on X-ray film (original size) and as enlargements (two times) on photographic paper.

The above mentioned collection will be supplemented with further examples of defects revealed by neutron radiography which were and will be contributed by other NRWG members. Then the revised version of the atlas will be published as a special Euratom document.

As it is difficult to reproduce in this publication all the neutron radiographs contained in the atlas, a selection was made of those enlargements from the atlas that illustrate the most characteristic defects occurring in light water reactor fuel.

At the First World Conference on Neutron Radiography a display will be made, consisting of a wall display and a audio-visual display.

The wall display contains a poster with the following: a schematic diagram of a nuclear fuel pin (in colours) showing its components in which defect may occur; 36 neutron radiographs from the collection (illuminated from the back) and a coloured diagram showing the classification of defects.

The audio-visual display consists of 81 slides, to be projected on a desk projector on which an endless magnetic tape is played, giving a sound commentary on each projected slide. The duration of the whole audio-visual cycle is 12 min.

---

\*) J.C. Domanus: Neutron Radiographic Findings in Light Water Reactor Fuel. Metallurgy Department. Risø National Laboratory. June 1979.

## INTRODUCTION

The assessment of neutron radiographs of nuclear fuel elements can be much easier, faster and simpler if reference can be made to typical defects, which can be revealed by neutron radiography.

In other fields of industrial radiography collections of reference radiographs, showing typical defects in welding, or casting have been completed and published long ago.

Since 1974 neutron radiography is routinely used at Risø National Laboratory for the quality and performance control of nuclear fuel. About 2000 neutron radiographs were taken, mainly during the post irradiation examination of light water reactor fuel.

During the assessment of neutron radiographs some typical defects of the fuel were found and it was felt that a classification of such defects will help to speed up the assessment procedure. Therefore an attempt was made to establish such a classification, which is currently used at Risø now. This classification is presented in this atlas.

**NOTE:** In the present collection of neutron radiographs the term "defect" is used for designation of a neutron radiographic finding, showing a different appearance of a particular part of the fuel from that, which will be shown on a neutron radiograph of that part as fabricated.

## FUEL PINS

For the purpose of the present collection of neutron radiographs a typical example of a nuclear fuel pin, used in light water reactors, was chosen.



Figure 1 shows all the components of such a fuel pin where defects, detectable by neutron radiography, can occur. Those components are marked with the following capital letters:

- Nuclear fuel: A.
- Fuel cladding: B.
- Plenum: C.
- End plugs: D.
- Instrumentation: - E.

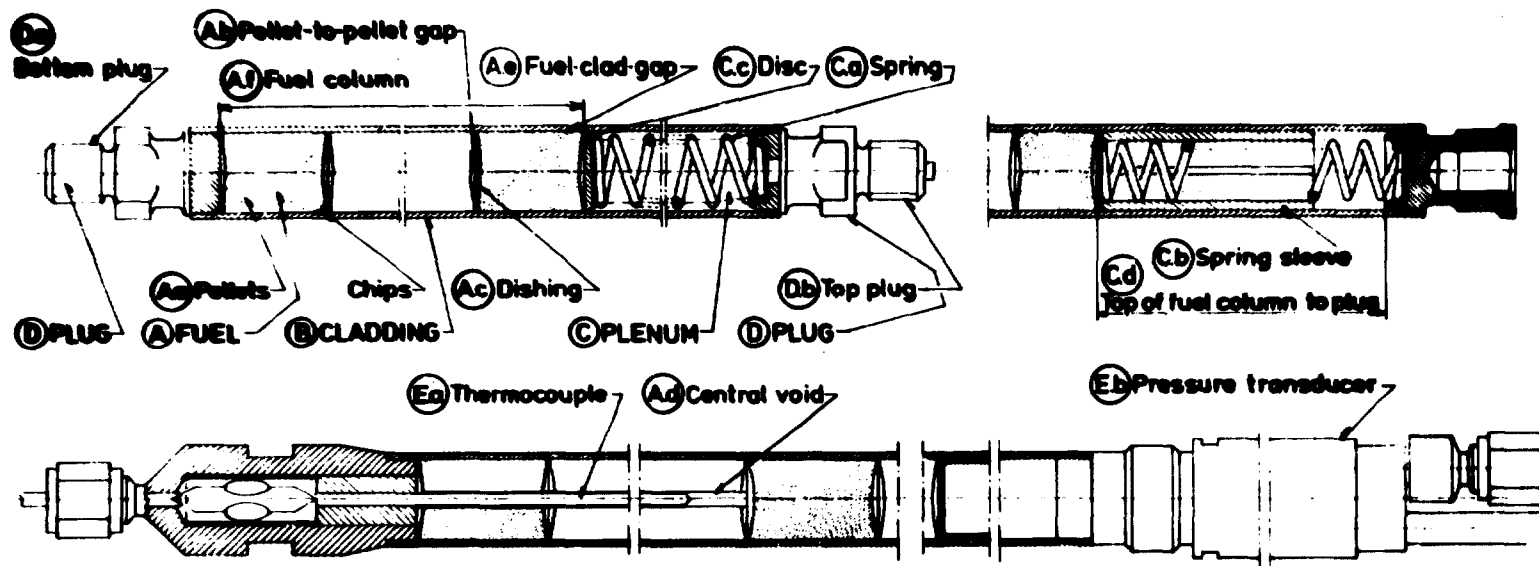


Fig. 1. Components of a typical nuclear pin.

### DEFECT LOCATION

On figure 2 fuel pin components (shown on fig. 1) are subdivided into elements where defects may occur (listed in the vertical column at the left and marked with small letters).

	Cracks												Chips							Dim.						
	1	2	3	4	5	6	7	8	9	10	11	12	13	14	15	16	17	18	19	20	21	22	23	24		
● Defects shown on display. ○ Defects occurring, but not shown. x Dimensions from neutron radiographs. ⊕ Dimensions measured at Rise. Defect intensity: 1 - small 2 - medium 3 - high	A	a Pellets	●	●	●	●	●	●	●	●	●	●	●	●	●	●	●	●	●	●	●	●	●	●	●	
		b Pellet-to-pellet gap	○																							
		c Dishing	○																							
		d Central void	○																							
		e Fuel-to-clad gap	○																							
		f Fuel column	○																							
		g Cladding	○																							
B	a Spring	○																								
	b Spring sleeve	○																								
	c Disc	○																								
C	d Top of fuel column to plug	○																								
	a Bottom end	○																								
D	b Top end	○																								
	a Thermocouple	○																								
E	b Pressure transducer	○																								
	c Other	○																								
F	a Longitudinal	○																								
	b Transverse	○																								
G	a Annular	○																								
	b Corner	○																								
H	a Other	○																								
	b In pellet-to-pellet gap	○																								
I	a In fuel-to-clad gap	○																								
	b Not present	○																								
J	a Enlarged	○																								
	b Contracted	○																								
K	a Filled up	○																								
	b Deformed	○																								
L	a In one pellet	○																								
	b Through sev. pellets	○																								
M	a Through whole fuel column	○																								
	b Different n-absorption	○																								
N	a Hydrides	○																								
	b Broken	○																								
O	a Dislocated	○																								
	b Expanded	○																								
P	a Diameter	x																								
	b Thickness	x																								
Q	a Length	x																								
	b	x																								

Fig. 2. Fuel pin components and defects occurring in them.

## DEFECT NATURE AND ORIGIN

Defects which may occur in different elements of the fuel pins can be of different nature and origin. They are listed at the top of figure 2 (columns 1 to 21).

## DIMENSIONS

It is also possible to measure dimensions from neutron radiographs. Therefore the last three columns (22 to 24) at the top of the figure 2 list those dimensions.

## DEFECTS OCCURRENCE

On the figure 2 the sign "." signifies, that in that location a particular defect can occur and that this defect is illustrated in the present collection.

There are, however, more defects which can most likely occur in nuclear fuel and can be detected by neutron radiography, but which were not found among the 2000 RISØ radiographs. They are marked with "o" on figure 2.

## MEASURING OF DIMENSIONS

Besides the defects, dimensions of various elements of the fuel pins can be determined from neutron radiographs. Those instances are marked with "x" on figure 2 and those which are routinely measured during the assessment of neutron radiographs at RISØ are marked with "ø".

## DEFECT INTENSITY

Defects in nuclear fuel can occur with different intensity (e.g. cracks in fuel pellets can be miniscule, slightly visible, or so big as to break the whole pellet). Therefore

it was felt that one shall also classify the intensity of the defects. For that purpose an arbitrary three grade scale was adopted: 1 - meaning small, 2 - medium and 3 - high intensity defect. This intensity classification is used routinely at RISØ for the assessment of defects revealed by neutron radiography.

#### CONTENTS OF THE COLLECTION

The collection of the atlas contains neutron radiographs of defects marked with "." on figure 2.

The original neutron radiographs were taken at the DR 1 RISØ reactor (2 kW) on double coated Agfa Gevaert Structurix D4 X-ray film. A transfer technique was used with a 0.1 mm dysprosium foil. Exposure time to a  $1.6 \times 10^6 \text{ n.cm}^2 \cdot \text{s}^{-1}$  neutron beam (10 x 10 cm) was about 30 min. The L/d ratio in the vertical direction of the neutron beam (perpendicular to fuel pin axis) was 110 and in the horizontal direction (coinciding with the pin axis) was 27.5.

The radiographs in the atlas are reproductions of the original neutron radiographs copied on Kodak X-Omat Duplicating Film.

The original neutron radiographs were also photographed on a 35 mm Agfapan 100 film and thereafter enlarged (twice) on photographic paper. These enlargements are also included in the atlas.

#### DEFECTS REVEALED BY NEUTRON RADIOGRAPHY

Defects revealed by neutron radiography can be located in the components of the fuel pins shown on figure 1. They are classified and illustrated in the atlas.

Copies of neutron radiographs (original size) on film as well as enlargements (two times) on paper are given there, too.

As mentioned before in the present publication only a selection of neutron radiographs is presented as enlargements on photographic paper.

#### HOW TO USE THE COLLECTION

The copies of the neutron radiographs on film can be viewed without removing them from the atlas against the blank page which follows the copy. This blank page shall be illuminated by a shaded desk lamp. Thus this lighted blank page will serve as an illuminator, against which the radiograph may be read without removing it from the collection.

The reference radiograph may also be removed from the collection and be viewed on an illuminator together with the actual radiograph under assessment.

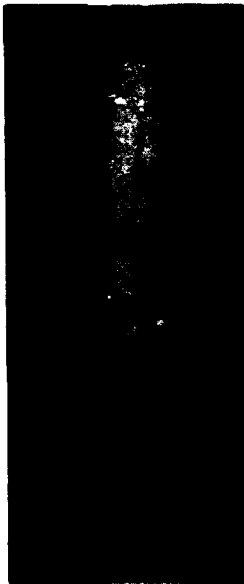
#### SELECTION OF CHARACTERISTIC DEFECTS

A selection of defects revealed by neutron radiography in light water reactor fuel is given below. Enlargements (two times) of neutron radiographs on photographic paper are reproduced. The defects location and their nature and origin are marked according to the classification adopted on fig. 2.

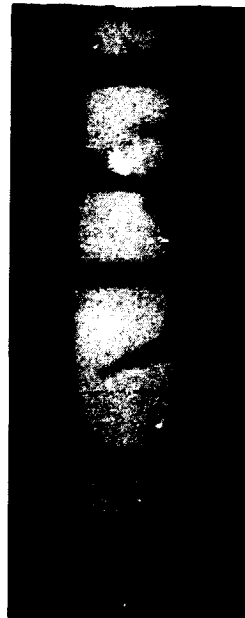
A. Defects in fuel

A.a. Defects in pellets

Cracks in pellets are illustrated in Fig. 3, whereas Fig. 4 shows chips of pellets.

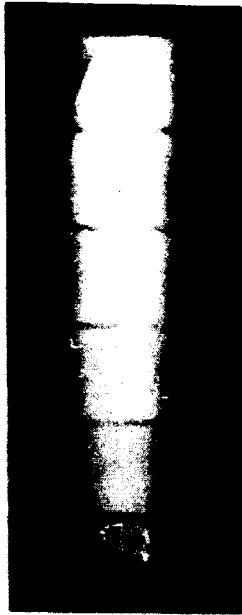


A.a.2 - Longitudinal cracks



A.a.3 - Transverse cracks

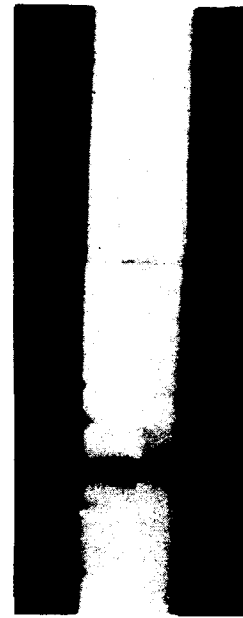
Fig. 3. Cracks in pellets.



A.a.5 - Corner chips



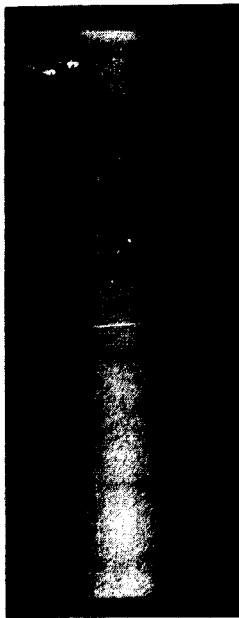
A.a.6 - Other chips



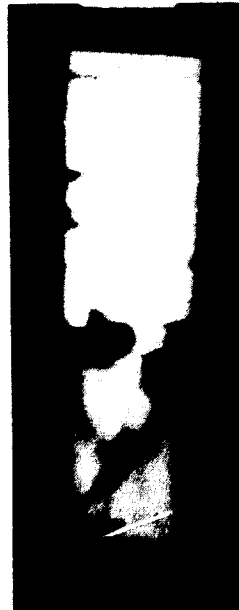
A.a.7 - Chips in pellet-to-pellet gap

Fig. 4. Chips of pellets.

On Fig. 5 enlarged and broken pellets are shown.



A.a.10 - Pellet enlarged



A.a.19 - Broken pellet

Fig. 5. Enlarged and broken pellets.

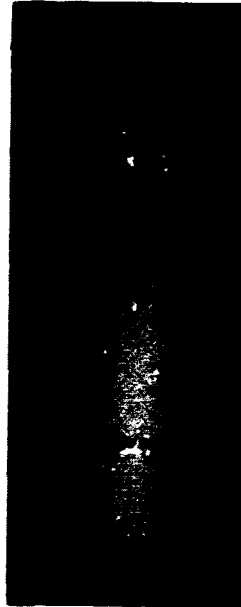


A.b. Defects in pellet-to-pellet gap

On Fig. 6 both an enlarged as well as an contracted pellet-to-pellet gap can be seen.



A.b.10 - Pellet-to-pellet gap enlarged

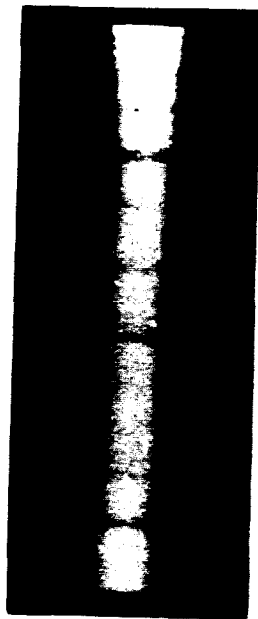


A.b.11 - Pellet-to-pellet gap contracted

Fig. 6. Pellet-to-pellet gap enlarged and contracted.

A.c. Defects in dishing

A filled up and deformed dishing can be seen on Fig. 7.



A.c.12 - Dishing filled-up



A.c.13 - Dishing deformed

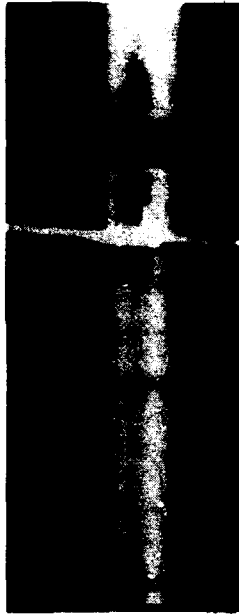
Fig. 7. Filled-up and deformed dishing.

A.d. Central void

Central void can be detected in one pellet or going through several pellets (as shown on Fig. 8) or can even go through the whole fuel column.



A.d.14 - Central void in one pellet



A.d.15 - Central void through several pellets

Fig. 8. Central void in one and in several pellets.

A.e. Defects of fuel-to-clad gap

Defects of fuel-to-clad gap are hard to detect and even harder to reproduce in print. Therefore no such example is given here.

B. Defects in cladding

B.a. Deformed and broken cladding

A deformed and broken cladding can be seen on Fig. 9.



B.a.13 - Cladding deformed



B.a.19 - Cladding broken

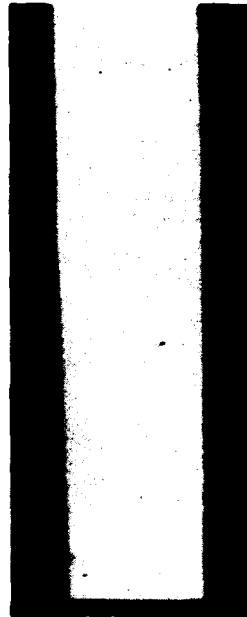
Fig. 9. Deformed and broken cladding.

B.a. Hydrides in cladding

Hydrides in cladding, although relatively easily detected on neutron radiographs can hardly be seen when reproduced in print. Fig. 10 shows some hydrides revealed in the cladding.



B.a.18 - Hydrides in cladding



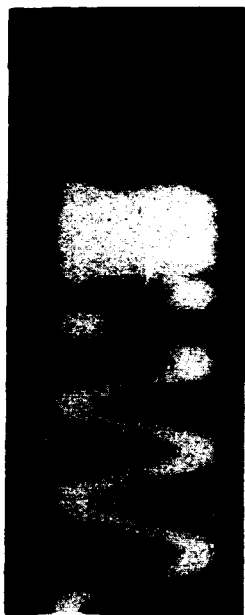
B.a.18 - Hydrides in cladding

Fig. 10. Hydrides in cladding.

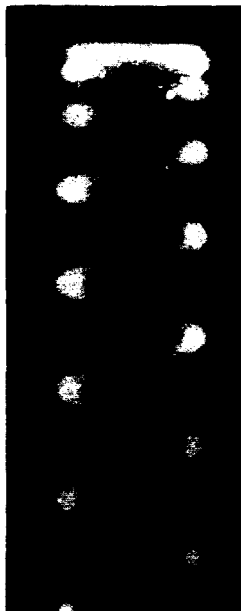
C. Defects in plenum

C.a. Defects of spring

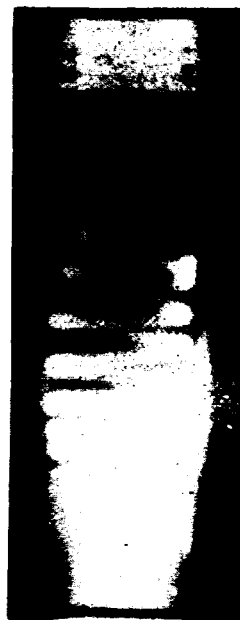
Different defects of the spring in plenum are illustrated on Fig. 11.



C.a.11 - Spring contracted



C.a.13 - Spring deformed

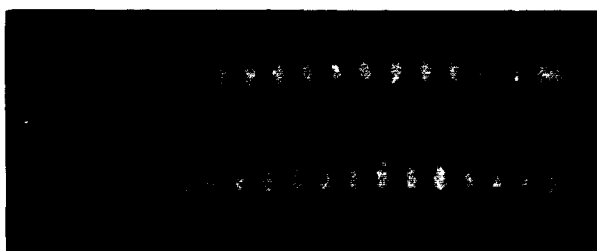


C.a.20 - Spring dislocated

Fig. 11. Defects of the spring in plenum.

C.b. Defects of spring sleeve

Fig. 12 illustrates a broken spring sleeve.



C.b.19 - Spring sleeve broken

Fig. 12. Broken spring sleeve.

**C.c. Disc**

The disc separating the spring of the plenum from the last (or first) pellet can be dislocated, as shown on Fig. 13.

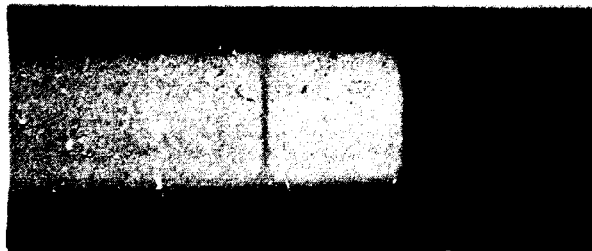


C.c.20 - Disc dislocated

Fig. 13. Dislocated disc.

**D. Defects in end plugs**

Fig. 14 illustrates hydrides detected in the bottom plug.



D.a.18 - Hydrides in plug

Fig. 14. Hydrides in the bottom plug.

Other defects can be detected by neutron radiography as well.

### E. Instrumentation

Defects in various instruments (e.g. thermocouples, pressure transducers) located in fuel pins can be revealed by neutron radiography. Fig. 15 gives an example of a dislocated thermocouple.



E.a.20 - Thermocouple dislocated

Fig. 15. Dislocated thermocouple.

#### DEFECTS NOT SHOWN IN THE PRESENT COLLECTION

In the atlas only those defects in nuclear fuel are shown which could be chosen from the neutron radiographs taken at the Risø National Laboratory. There are, however, more defects which can most likely occur in nuclear fuel and can be detected by neutron radiography. Those defects were marked with "o" on figure 2. It is also possible to find some other typical defects in nuclear fuel worth including in this collection.

Therefore all persons in possession of such neutron radiographs, missing in this collection, are kindly asked to supply them to:

Risø National Laboratory  
Metallurgy Department  
DK-4000 Roskilde  
Denmark

They will be included in the next edition of the atlas.



SEARCH FOR ADEQUATE QUALITY STANDARDS  
FOR NEUTRON RADIOGRAPHY OF NUCLEAR FUEL

J.C. Domanus  
Nuclear Department  
Elsinore Shipbuilding & Engineering Co. Ltd.\*)  
DK-3000 Helsingør, Denmark

ABSTRACT

Unlike in other fields of industrial radiography, where standard methods and procedures are used to control the quality of the radiographic image, no such standard exist for neutron radiography of nuclear fuel. To fill that gap it was felt that standardization work ought to be started in that field, too. According to that in 1979 an Euratom Neutron Radiography Working Group was constituted, which initiated standardization work in the field of neutron radiography of nuclear fuel. Finding adequate standards for image quality of neutron radiographs and checking the accuracy of dimension measurements from them were given first priority. The only existing standard in the field of neutron radiography (ASTM E 547-77 [1] now under revision) was applied to the control of quality of neutron radiographs of nuclear fuel elements and proved to be inadequate. Therefore different design of beam purity and sensitivity indicators were envisaged, discussed and analysed by the NRWG and finally produced, to be tested under a special test program [3]. The separate problem of testing the accuracy of measurement of different dimensions of nuclear fuel pins from neutron radiographs is under consideration by the NRWG. Preliminary investigations [2] have shown that this problem can be solved by the use of calibration fuel pins, simulating the true nuclear fuel pins and containing such calibrated items as fuel-to-clad gaps, pellet-to-pellet gaps, central voids, dishings. By the use of such calibration fuel pins accuracy of dimension measurements will be tested under the same test program as mentioned above. Neutron radiographs of the calibration fuel pins will be also used to assess adequacy of use of various measuring instruments and methods. It is hoped that the results of this search will permit to develop standard methods, with the use of which the quality of neutron radiographs of nuclear fuel could be assessed and information obtained whether the neutron radiographic facility in question does fulfill minimum requirements set up by the standard. It is also hoped that best dimension measuring methods will be chosen and equipment improved.

---

\*) Work performed under contract with Risø National Laboratory.

## INTRODUCTION

Like in other fields on industrial radiography, in neutron radiography of nuclear fuel, standardization is necessary to be able to use recognized methods for the control of radiographic image quality as well as procedures which will assure that the prescribed quality can be obtained. Having this in mind standardization work was initiated within Euratom to cope with the different problems of neutron radiography of nuclear fuel elements. Present status of work in this field is reviewed.

Neutron radiography is a well established technique within non-destructive testing control. One of the areas in which it is mostly used is the pre- and especially post-irradiation control of nuclear fuel elements. In other fields of industrial radiography standard methods and procedures are used to control the quality of the radiographic image. Standard reference radiographs, showing typical defects revealed by radiography are also used. It is felt that similar standardization is needed for neutron radiography. Unfortunately nearly none of such standards exist in this field. Therefore standardization work ought to be started and Risø National Laboratory has proposed to establish a working group within Euratom. At the first Euratom meeting on neutron radiography, held at Risø in May, 1979, following items were considered as having the first priority for standardization: 1) Radiographic quality indicators. 2) Classification of defects. 3) Recommended radiographic practices. 4) Terminology. 5) Accuracy of dimension measurements. 6) Optimum conditions for nitrocellulose film. Work on some of the above items was started and is described below.

For the sake of testing the radiographic image quality and accuracy of dimension measurements from neutron radiographs of reactor fuel, the NRWG has decided to produce and test special indicators developed for that purpose.

In the preliminary investigation it was determined that there are no suitable indicators prescribed in the existing standards on neutron radiography. The only published standard in that field [1], the ASTM E 545-75, was prepared for general neutron radiography and is now under revision.

Taking into account the work done on this revision as well as different proposals made by the NRWG members, it was decided to produce the following indicators for neutron radiography of nuclear fuel:

- Beam Purity Indicator BPI.
- Beam Purity Indicator Fuel BPI-F.
- Sensitivity Indicator SI.
- Calibration Fuel Pin CFP-E1.

Those indicators, fabricated at Risø National Laboratory, were distributed among all NRWG participants and will be tested under a special NRWG Test Program [2]. The design of the



Key feature of the device is the ability to make a visual analysis of its image for subjective quality information. Densitometric measurements of the image of the device permit quantitative determination of radiographic contrast, low energy gamma contribution, pair production contribution, image unsharpness, and information regarding film and processing quality.

Beam Purity Indicator-Fuel BPI-F

For controlling the neutron beam components in nuclear fuel radiography the NRWG has developed a special Beam Purity Indicator-Fuel, which is a modification of the ASTM BPI. (see Fig. 2.).

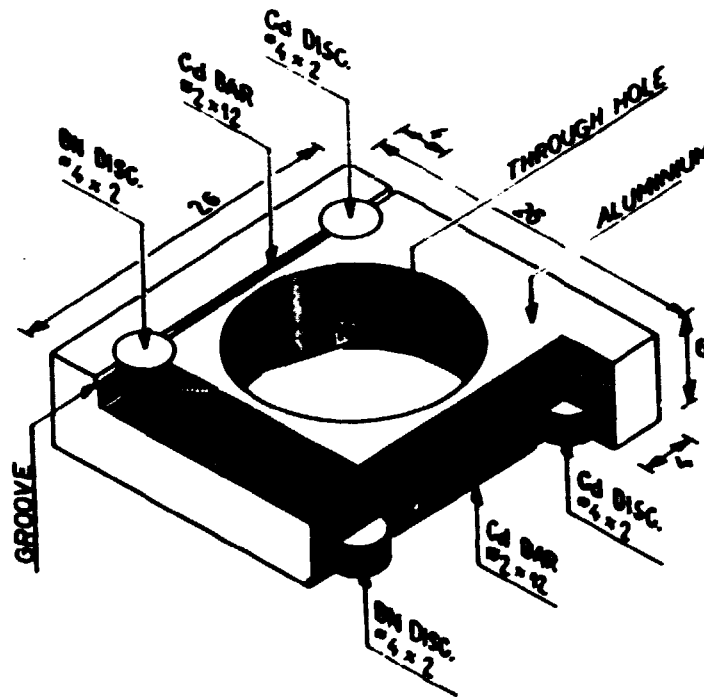


Fig. 2. Beam Purity Indicator-Fuel BPI-F.

The reasons behind the modification of the ASTM BPI are explained by R.S. Matfield as follows:

"The materials of the ASTM BPI were principally chosen to be suitable for the detection of gamma rays and as it is assumed that when the BPI-F is in use a transfer or track etch technique will be used, clearly a sensitivity to gammas is not needed. It is therefore considered that the base material

should be aluminium and that the filter-discs should be boron nitride and cadmium (the ASTM design has boron and lead discs)".

To be able to identify the exact location of the BPI and BPI-F on neutron radiographs one corner of the indicator was cut off (not shown on fig. 1 and 2).

From measurements of film densities under different parts of the BPI and BPI-F, and background density, different neutron beam components can be calculated.

The cadmium wire or rods included in each beam purity indicator are used to provide an indication of inherent beam resolution or sharpness.

### SENSITIVITY INDICATOR

Instead of the former four types of ASTM Sensitivity Indicators /I7 one new type of SI was developed. It is shown in fig. 3.

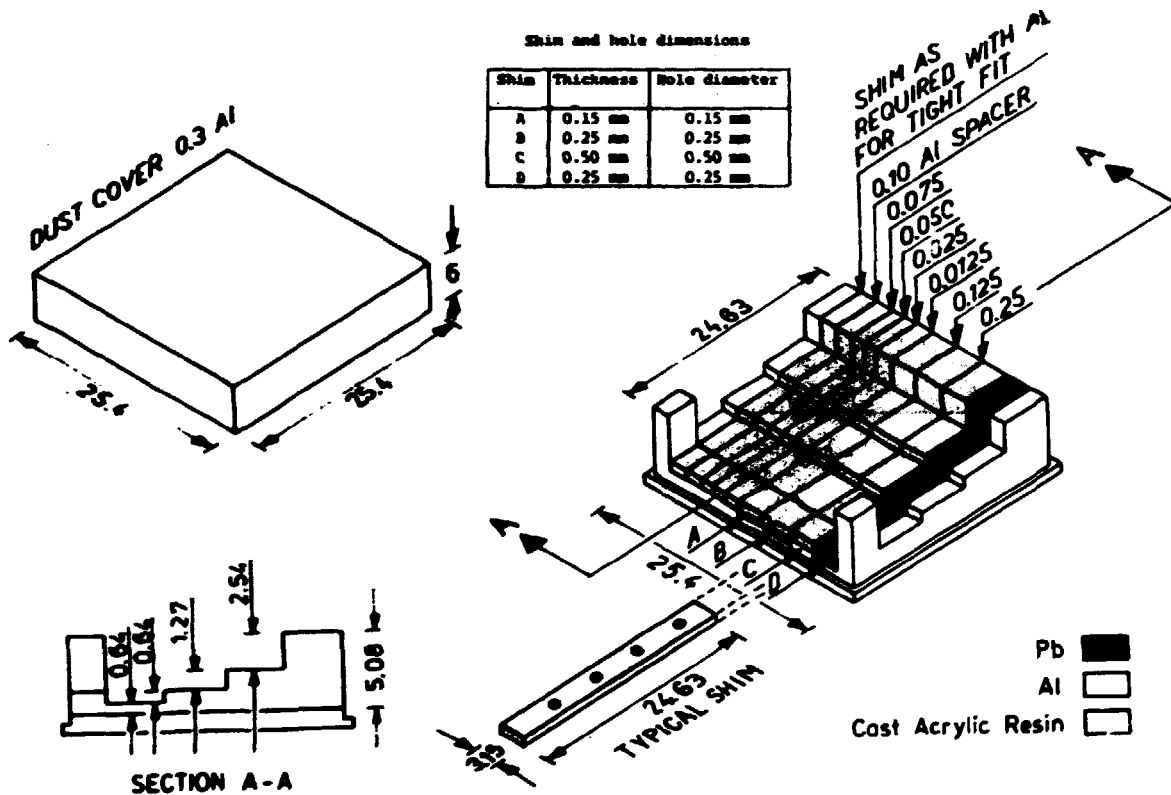


Fig. 3. The ASTM Sensitivity Indicator.

This sensitivity indicator basically combines a hole guage and gap gauge into a small single device. The holes are sized to be smaller than can be seen by conventional neutron radiography, and they progress up in size. Similarly, the gaps, formed by aluminium shims between sheets or acrylic resin, cover a range that is useful for all facilities.

The NRWG has considered a special design of a sensitivity indicator, including steps and shims of  $UO_2$ , which could be useful in evaluating the image quality of neutron radiographs of nuclear fuel. Unfortunately, it is not technically feasible to construct such an indicator and therefore the ASTM SI was adopted by the NRWG for its Test Program.

#### CALIBRATION FUEL PIN

As mentioned in /17: "It is recognized that the only truly valid sensitivity indicator is material or component, equivalent to the part being neutron radiographed, with a known standard discontinuity (reference standard comparison part)".

Such a "reference standard comparison part" for nuclear fuel pin is the calibration fuel pin CFP-E1. It is shown on fig. 4.

According to the specifications given on fig. 4, 10 calibration fuel pins were produced at Risø and distributed among the NRWG members to be tested under the Test Program /27.

#### CONCLUSIONS

The beam purity indicators (BPI and BPI-F), sensitivity indicators (SI) and calibration fuel pins (CFP-E1) fabricated at Risø, were sent to all members of the NRWG. They will be tested under a special NRWG Test Program /37. Following its completion conclusions will be drawn about the adequacy of using of the particular indicators as quality standards for neutron radiography of nuclear fuel.

It will also be possible to draw conclusions on the best methods and instruments to be used for accurately measuring the dimensions of nuclear fuel components from neutron radiographs.

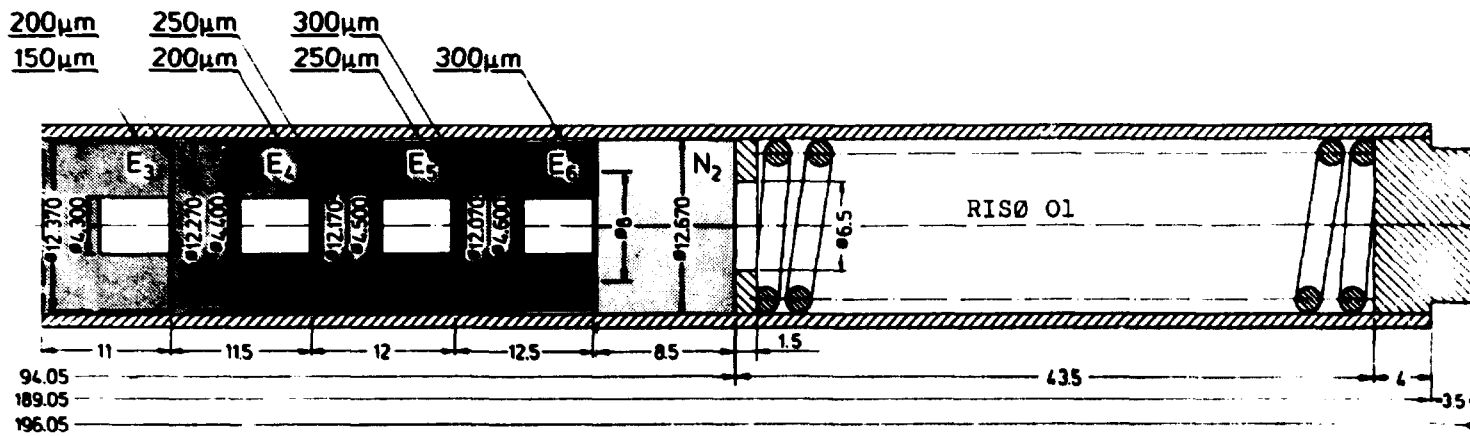
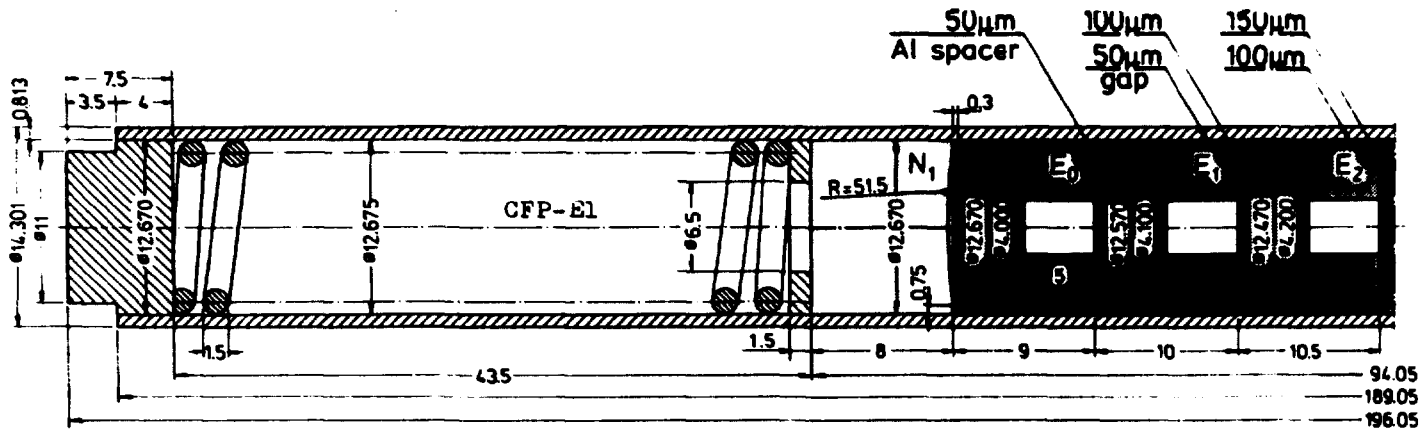


Fig. 4. Calibration Fuel Pin CFP-E1.

#### REFERENCES

- 11 ASTM E 545-75. Standard method for determining image quality in thermal neutron radiographic testing.
- 12 DOMANUS J.C. - Accuracy of dimension measurements from neutron radiographs of nuclear fuel pins. Rise-M-1860. 26.03.1976 and Eight world Conference on Nondestructive Testing. Cannes, 6-11.09.1976. Paper 3L-8.
- 13 DOMANUS J.C. , Euratom Test Program for image quality and accuracy of dimensions. WCNR, San Diego, 7-10.12.1981.



EURATOM TEST PROGRAM  
FOR IMAGE QUALITY AND ACCURACY OF DIMENSIONS

J. C. Domanus  
Nuclear Department  
Elsinore Shipbuilding & Engineering Co. Ltd. \*)  
DK-3000 Helsingør, Denmark

ABSTRACT

The Neutron Radiography Working Group constituted within Euratom in 1979 has developed a test program for checking the image quality and accuracy of dimensions measured from neutron radiographs of nuclear fuel pins. For that program specially designed and produced at Risø: calibration fuel pin beam purity indicators and sensitivity indicator will be used. They will be neutron radiographed together at each of the neutron radiography centers, participating in the NRWG. Silver halide X-ray films will be exposed with Gd and Dy converters by the direct and transfer method. Nitrocellulose film coated on both sides with a converter and without coating, but between two converter screens, will also be used. The radiographs will thereafter be processed at the centers themselves as well as at Risø. The results will be compared and conclusions drawn about the suitability of the test items for the purpose of assessing the neutron beam constituents, the image quality and the accuracy of dimension measurements.

---

INTRODUCTION

Already at its first meeting in 1979 the NRWG recognised the necessity of testing image quality indicators in search of adequate quality standards for neutron radiography of nuclear fuel. The only existing indicators at that time were the ASTM [1] indicators and a preliminary test program was elaborated at Risø. In view of the forthcoming revision of the ASTM standard this program has been revised, too. Following the discussions between the members of the NRWG and after two consensive meetings of the NRWG (in 1980 and 1981) a final test program has been developed and adapted for extention. For that program beam purity and sensitivity indicators as well as a calibration fuel pin were fabricated at Risø on behalf of Euratom. They are described in detail in [2]. All those test items were sent to all 10 NRWG members and will be tested according to the program described below.

---

\*) Work performed under contract with Risø National Laboratory.

## ITEMS FOR THE TEST PROGRAM

Following test items have been fabricated at Risø:

- Beam Purity Indicator BPI (according to the revised ASTM specification). (See fig. 1).
- Beam Purity Indicator-Fuel BPI-F (according to the design proposed by R. S. Matfield, member of the NRWG). (See fig. 2).
- Sensitivity Indicator SI (according to the revised ASTM specification). (See fig. 3).
- Calibration Fuel Pin CFP-E1 (according to the Risø design, based on previous investigation [3]). (See fig. 4).

## MATERIALS FOR THE TEST PROGRAM

All the NRWG participants have received the following material on which the test program will be performed:

- X-ray film: Kodak Industrex M and SR, Agfa-Gevaert Structurix D4.
- Nitrocellulose film: Kodak-Pathé CN85 and CN 85B.
- Metal converter screens: Gadolinium 25  $\mu\text{m}$  and dysprosium 100  $\mu\text{m}$ .
- Boron converter screens: Kodak-Pathé BN1.
- High contrast film (for copying nitrocellulose radiographs): Kodak SO-015.
- Polarising filters (for direct evaluating nitrocellulose radiographs): Polaroid Polariser HNCP-STD, 0.03".

## DETECTION SYSTEMS

During the investigation two detection systems will be used. One consisting of a metal conversion screen and a silver halide film and the other of the nitrocellulose film coated on both sides with a conversion screen (or a nitrocellulose film and two separate conversion screens). Both systems are described below.

### Metal Conversion Screens and Silver Halide Films

Metal conversion screens and silver halide films are used with both the direct as well as the transfer method of neutron radiography.





In both methods single coated and double coated X-ray films will be tested.

While testing the indicators by the direct method the 25  $\mu\text{m}$  thick gadolinium conversion screens will be used, whereas for the transfer method the 100  $\mu\text{m}$  thick dysprosium conversion screen will be used.

#### Nitrocellulose Film

Nitrocellulose films for neutron radiography must be used with conversion screens. Those conversion screens are either used as a coating on the nitrocellulose film or as separate screens.

As nitrocellulose film the CN85 (colourless) film will be used. It can be coated on both sides with the conversion screens and in this case it is called CN85 type B film. The coating consists of lithium borate dispersed in a water-soluble binder.

Nitrocellulose film CN85 can be used with separate conversion screens BN 1 made from natural boron.

#### EXPOSURE TECHNIQUE

The calibration fuel pin CFP-E1 will be radiographed together with all the three indicators: BPI, BPI-F and SI.

For the purpose of determining image quality on silver halide films the background density closest to the area of interest shall be about 2.0. Background film density variation across the film shall not exceed 10% ( $\pm$  5%) variation from the numerical mean of five measurements: one measurement at the center and one measurement toward the center from each corner.

Exposures to neutrons shall thus be chosen accordingly, to reach those densities.

The densities reached on nitrocellulose film depend not only on the exposure to neutrons but also on the etching conditions. The nitrocellulose films shall be etched in a 10% (2.5N) solution of analytical grade sodium hydroxide. During a common investigation performed by the research laboratories of Kodak-Pathé and by Risø it was found that best results are reached while etching the films for 45 min at 50°C (Kodak) and for 21 h at 20°C (Risø).

It is hard to recommend exact exposures to neutrons. According to the experience reached so far at Risø with the use of nitrocellulose film it was found that satisfactory results are reached when nitrocellulose CN85 type B films are exposed about three times longer to neutrons than the D4 film, or as long as the single coated SR film, with the Dy transfer technique. It is common practice to copy neutron radiographs taken on nitrocellulose film into high contrast graphic film. Thus the assessment of neutron radiographs is much easier. For that purpose the

Kodak Kodalith graphic film was normally used. This, however, produces a negative copy of the nitrocellulose original and from such a copy the BPI's cannot be evaluated. Therefore it is better to make the copy from a nitrocellulose film on a Kodak SO-015 Duplication film, which supersedes the Kodatone film and gives a positive copy, suitable to direct evaluation.

#### TEST PROGRAM

The best conditions for a direct comparison of test results can be reached when all the films exposed to neutrons will be processed at one facility (preferably at the same time) using the same processing conditions. Therefore it is proposed that at each neutron radiography facility, participating in the program, two sets of each neutron radiograph will be produced: one to be processed at that facility (using their routine procedure) and one to be sent to Risø for processing (by a standard processing procedure).

Having this in mind as well as all that which has been mentioned above, following test program is proposed.

Table 1. Test Program

Film	Screen	Method	Processing		Copy
			at	conditions	
SR	Gd	direct	Site	routine	-
SR	Gd	direct	Risø	standard	-
D4	Gd	direct	Site	routine	-
D4	Gd	direct	Risø	standard	-
M	Gd	direct	Site	routine	-
M	Gd	direct	Risø	standard	-
SR	Dy	transfer	Site	routine	-
SR	Dy	transfer	Risø	standard	-
D4	Dy	transfer	Site	routine	-
D4	Dy	transfer	Risø	standard	-
M	Dy	transfer	Site	routine	-
M	Dy	transfer	Risø	standard	-
CN85-B	-	-	Site	routine	routine
CN85-B	-	-	Risø	20°C, 21 h	SO-015
CN85-B	-	-	Risø	50°C, 45 min	SO-015
CN85	BN1	-	Site	routine	routine
CN85	BN1	-	Risø	20°C, 21 h	SO-015
CN85	BN1	-	Risø	50°C, 45 min	SO-015

#### ASSESSMENT OF TEST RESULTS

Different values retrieved from neutron radiographs of the BPI, BPI-F, SI and CFP-E1 shall be assessed separately.

### Neutron Exposure Contributions

By measuring film densities (of the silver halide film) under different parts of the BPI or BPI-F, different values of neutron exposure contributions can be determined. Table 2 gives the film densities from which different boron contents can be calculated (as in table 3).

Table 2. Film Densities Under Different Parts of BPI and BPI-F  
(See fig. 1 and 2)

Film density under	BPI	BPI-F
Lower BN disc	$D_1$	$D_D$
Upper BN disc	$D_2$	$D_C$
Lower Pb disc	$D_3$	-
Upper Pb disc	$D_4$	-
Upper Cd disc	-	$D_E$
Lower Cd disc	-	$D_F$
Teflon body	$D_6$	-
Center of hole	$D_5$	$D_B$

Table 3. Neutron Exposure Contributions

Calculated content	BPI	BPI-F
Thermal neutron	$[D_5 - (\text{higher value of } D_1 \text{ \& } D_2)]:D_5$	$(D_B - D_E):D_B$
Scattered neutron	$(D_1 - D_2):D_5$	$(D_C - D_D):D_B$
Ephithermal neutron	-	$(D_E - D_C):D_B$
Gamma	$[D_6 - (\text{lower value of } D_3 \text{ \& } D_4)]:D_5$	-
Pair production	$(D_3 - D_4):D_5$	-

### Image Sharpness

Besides the above mentioned density measurements and calculations from the radiograph of the BPI and BPI-F one shall further visually compare the images of the cadmium rods or bars in the beam purity indicator. An obvious difference in image sharpness indicates an L/D ratio which is probably too low for general inspection. Detailed analysis of the rod images is possible using a scanning microdensitometer.

### Sensitivity Indicator

The purpose of the sensitivity indicator (see fig. 3) is to determine the sensitivity of details visible on the neutron radiograph by evaluating the neutron radiographic image of the SI.

Besides one shall visually inspect the image of the lead

steps in the sensitivity indicator. If the 0.25 mm holes are not visible, the exposure contribution from gamma radiation is very high and further analysis should be made.

When examining the neutron radiographs of the SI one shall visually inspect the image of the cast acrylic resin steps and note all the holes visible to the observer (consecutive holes marked as H). Then one shall take as the value of H reported, the largest consecutive value of H that is visible in the image.

The cast acrylic resin steps, shown on the left side of the SI are separated by aluminium spacers with thickness (gap size) marked as G.

During the visual examination of the neutron radiograph of the SI one shall report the G value. The value of G reported is the smallest gap which can be seen at all absorber thicknesses.

#### Image Quality Levels

The thermal neutron content, scattered neutron content, gamma content, and pair production content are determined by densitometric analysis of the image of the beam purity indicator with subsequent calculations. Sensitivity level is determined by visually analyzing the image of the sensitivity indicator and subsequently determining the values of H and G.

The designation of quality level shall include thermal neutron content (NC) and sensitivity level. The designation shall be NC-H-G. Values for scattered neutron content, gamma content, and pair production content may also be specified.

#### Calibration Fuel Pin CFP-E1

From the neutron radiographs of the CFP-E1 (see fig. 4) following dimensions ought to be determined.

Axial dimensions (read along the longitudinal axis of the pin).

- Total fuel stack length.
- Length of all pellets.
- Length of the central void.
- Dishing between pellets  $N_1$  and  $E_0$ .
- Pellet-to-pellet gaps.

Radial dimensions

- Pellet diameters of nonstepped pellets.
- Pellet diameter of stepped pellets.
- Pellet-to-pellet gaps.



- Cladding tube wall thickness.
- Central void diameter.

All the above mentioned measurements will be performed using those measuring instruments (e.g. scanning microdensitometer, projection microscope) available at the particular centers.

From neutron radiographs of the CFP-E1 both axial as well as radial dimensions can be read. The results of those measurements shall be compared with the true dimensions as given in the CFP-E1 certificate.

#### FINAL REMARKS

As stated in the ASTM [1] standard: "Metal conversion screens and silver halide film were used in the development and testing of the beam purity indicator". Therefore it is not clear whether it will be possible to use the BPI and BPI-F also with the nitrocellulose film and its converter screens. It seems possible, that while using the polarized filters in directly evaluating the nitrocellulose film the same technique of evaluating the results obtained with the use of the BPI and BPI-F will be applicable.

One of the purposes of the NRWG test program is to determine the usefulness of all the indicators in neutron radiography of nuclear fuel taken both on silver halide as well as on nitrocellulose film.

#### REFERENCES

- [1] ASTM E545-75. Standard method for determining image quality in thermal neutron radiographic testing.
- [2] DOMANUS, J. C., Search for adequate quality standards for neutron radiography of nuclear fuel. WCNR, San Diego, 7-10.12.1981
- [3] DOMANUS, J. C., Accuracy of dimension measurements from neutron radiographs of nuclear fuel pins. Risø-M-1860. 26.03.1976 and Eight World Conference on Nondestructive Testing. Cannes, 6-11.09.1976. Paper 3L-8.

**HOW GOOD IS NITROCELLULOSE FILM  
FOR NEUTRON RADIOGRAPHY?**

J. C. Domanus  
Nuclear Department  
Elsinore Shipbuilding & Engineering Co. Ltd. \*)  
DK-3000 Helsingør, Denmark

**ABSTRACT**

A comparison was made of radiographic quality and sensitivity of neutron radiographs taken on silver halide and nitrocellulose film. For the quality comparison a special calibration fuel pin was used, containing calibrated fuel-to-clad gaps between the  $UO_2$  pellets and zircaloy cladding tube. The neutron radiographs of this pin were assessed by three observers for radiographic image quality referred to X-ray radiographs of the pin.

The radiographic sensitivity was investigated with ASTM E 545 sensitivity indicators and assessed in the same way as the calibration fuel pin.

As the neutron radiographs taken on nitrocellulose film are usually not directly assessed from the original nitrocellulose film but from their copies during the investigation the nitrocellulose films were copied on high contrast graphic film (Kodalith), direct reversal film (Kodatone), and enlarging paper (Kodabrom). They were also viewed through polarising filters.

Results of the quality and sensitivity assessment done for the nitrocellulose film by the methods described above were compared with those for the silver halide film used in the direct and transfer neutron radiography of the same objects.

---

**INTRODUCTION**

The problem of accurate dimensional measurements from neutron radiographs of nuclear fuel pins [1] as well as that of attaining the best quality nuclear fuel radiographs [2] have been studied at Risø for some time. For those studies a special calibration fuel pin has been designed and fabricated (as described in [1]) by means of which both the accuracy of dimensional measurements as well as the radiographic image quality of neutron radiographs can be assessed (this calibration fuel pin was later redesigned and produced as described in [3]).

In the former investigation both the Kodak-Pathé CA80-15B and CN85B nitrocellulose film were irradiated and assessed by the direct evaluation method. The CN85B film (the CA80-15B is no longer manufactured) was studied from the point of view of radiographic quality.

As in routine neutron radiography, radiographs taken on

---

\*) Work performed under contract with Risø National Laboratory.

nitrocellulose film are very seldom assessed by the direct visual method. Thus, the CN85B radiographs were assessed both directly from CN85B radiographs as well as from copies made on Kodalith and Kodatone film and Kodabrom paper. They were also assessed by viewing the CN85B radiographs through polarizing filters.

To take the different irradiation conditions to neutrons into account the calibration fuel pin was radiographed both at the Risø DR1 reactor (details of this facility can be found in [4 and 5]) and the Triton reactor at Fontenay-aux-Roses, France, (details of this facility can be found in [6]).

One set of neutron radiographs taken at Risø was processed there, whereas a second set was sent to Kodak-Pathé for processing. The Fontenay-aux-Roses radiographs were also processed at Kodak-Pathé.

The assessment of all neutron radiographs (and copies thereof) was made at Risø.

For the sake of comparison with silver halide films neutron radiographs of the same calibration fuel pin were also taken on such films both at Risø and Fontenay-aux-Roses and were thereafter assessed in the same way as the nitrocellulose film.

The neutron radiographs of the calibration fuel pin were taken together with the ASTM sensitivity indicators [7]. The assessment of those neutron radiographs was also made at Risø, but is not reported here, as both ASTM and Euratom [3] have decided to use a sensitivity indicator of a different design.

## EXPERIMENTAL TECHNIQUE

### Test Objects

As a test object, the calibration fuel pin KBS-3 (described in [1] and shown schematically on fig. 1) was used. It consisted of two  $UO_2$  pellets of natural uranium and six  $UO_2$  pellets

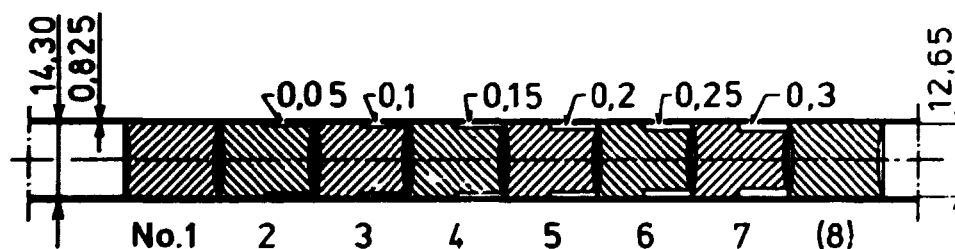


Fig. 1. Calibration fuel pin KBS-3.

of enriched uranium. All pellets were enclosed in a zircaloy tube. The diameter of the two  $UO_2$  pellets made of natural uranium fits closely to the inner diameter of the cladding tube, whereas the remaining six pellets in half of their length have the same diameter as the two end pellets (made of natural U), and have the second half ground down in such a way as to form pellet-to-clad gaps with dimensions shown in fig. 1 (from 50 to 300  $\mu m$ ).

It was mainly the sharpness of those gaps visible on neutron radiographs that was taken into account in assessing the quality of the neutron radiographs of the KBS-3.

As mentioned before, the ASTM [7] sensitivity indicators were exposed together with the KBS-3, but the results attained with them are not described in this report.

#### EXPOSURE TECHNIQUE

Both at Risø and at Fontenay-aux-Roses the same exposure to neutron technique was applied as used in routine neutron radiography at those facilities. To improve collimation conditions at Risø DRI facility an additional set of exposures was made using an increased (by 1 m) source-to-film distance.

Table 1 summarizes the exposures used for nitrocellulose and silver halide films.

Table 1. Exposures to neutrons

Film and Screen	Risø DRI		Fontenay-aux-Roses
	0 m	+ 1 m	Triton
CN85B	1.5 h	4.5 h	8 min & 16 min
D4 & Dy	15 min	45 min	30 min
M & Dy	-	-	30 min
R & Dy	-	-	30 min
T & Dy	-	-	30 min
SR & Gd	8 min	24 min	-
M & Gd	-	-	2.5 min
R & Gd	-	-	3 min
T & Gd	-	-	40 s

#### Films, screens, and processing technique

##### Nitrocellulose Film

As mentioned earlier Kodak-Pathé CN85B nitrocellulose film was used throughout the investigation. It consists of a 100  $\mu$ m thick film of cellulose nitrate, coated on both sides with lithium borate dispersed in a water-soluble binder, which acts as a converter screen by means of the (n,  $\alpha$ ) reaction.

The tracks detected by the film are not directly visible but have to be intensified by processing the film in the alkaline bath. A 10% (2.5N) solution in distilled water of caustic soda (sodium hydroxide) was used as the etching agent.

One set of neutron radiographs of the KBS-3, taken at Risø, was etched there at 20°C for 21 h, whereas the second set was sent to Kodak-Pathé, where it was etched at 50°C for 45 min. All radiographs taken at Fontenay-aux-Roses were etched at Kodak. It was previously found at Risø and at Kodak that the above-mentioned etching conditions give the best results.

##### Silver Halide Films

For the sake of comparison neutron radiographs were also taken on silver halide films, using both the direct technique with gadolinium screens and the transfer technique with the dysprosium screens. Details about the films and screens used are given in table 1. The films were processed according to the recommendations of the film manufacturers.

### Assessment of image quality

Different methods and instruments which can be used to assess the accuracy of dimensional measurements from neutron radiographs described previously in [1] were investigated. They can also be used to assess the image quality by e.g. measuring the pellet-to-clad gaps on the neutron radiographs and comparing the results with the physical dimensions of those gaps. Sensitivity indicators can also be used, and the ASTM [7] sensitivity indicators were actually used for that purpose. However, as the ASTM, as well as Euratom [3] is now introducing a new design for the sensitivity indicators, the overall quality of the neutron radiographs was assessed only by the use of the KBS-3 (the assessment of the quality by the use of the new sensitivity indicators as well as a new calibration fuel pin [3] will be made later). This represents the practical approach of assessing the quality of neutron radiographs of nuclear fuel pins as in routine radiography the radiographs are finally assessed by direct viewing done by the user of neutron radiography.

The overall image quality of the neutron radiographs of the KBS-3 was assessed by three observers. An arbitrary scale from 1 to 5 was used (1-very bad; 2-bad; 3-fair; 4-good; 5-very good). To produce radiographs of the KBS-3 indicating the gaps with the highest resolution X-ray radiographs (on D4, M and SR films) at 140 kV were made and their quality was rated as 5.

### Nitrocellulose Film

The radiographs on nitrocellulose film were assessed first directly and then through polarized filters (as recommended by Kodak-Pathé). Thereafter, copies of the nitrocellulose radiographs were made on high-contrast graphic film (Kodalith) as well as reversible Kodatone film (now superseded by Kodak SO-015 film). Finally, copies on photographic paper (Kodabrom) were made by means of an ordinary photographic enlarger (using a 1:1 enlargement) as contact copies give poorer results.

### Silver Halide Film

The radiographs on silver halide films were assessed directly with a high-illumination viewer and magnifying (2.5x) binoculars.

## RESULTS OF THE INVESTIGATION

As mentioned above, three persons have assessed the quality of the KBS-3 neutron radiographs using an arbitrary scale of 1 to 5. Only those results were taken into consideration for which all three persons gave the same valuation of image quality.

The results for nitrocellulose CN85B film are summarized in fig. 2, whereas fig. 3 gives the results for silver halide films.

		Quality	R-R		R-K		T-K-K		T-K-R	
			0 M	1 M	0 M	1 M	8 MIN	16 MIN	8 MIN	16 MIN
CN	5									
	4									
	3		X	X	X					
	2	X	X	X	X	X	X	X	X	X
PF	5									
	4									
	3	X	X	X	X					
	2	X	X	X	X	X	X	X	X	X
KL	5									
	4			X	X					
	3		X	X	X			X		
	2	X	X	X	X	X		X	X	X
KT	5									
	4		X	X						
	3	X	X	X				X		
	2	X	X	X		X		X	X	X
KB	5									
	4									
	3	X	X	X	X					
	2	X	X	X	X	X		X	X	X
	5									
	4									
	3	X	X	X	X					
	2	X	X	X	X	X		X	X	X
	5									
	4									
	3	X	X	X	X					
	2	X	X	X	X	X		X	X	X

Fig. 2. Image quality of KBS-3 neutron radiographs on nitro-cellulose film.

R-R: radiographed, etched (20°C, 21 h), and copied at Rise. R-K: radiographed at Rise, etched (50°C, 45 min) and copied at Kodak. 0 M: radiographed with a L/d=110. 1 M: radiographed with a L/d=160. T-K-K: radiographed at Pontenay-aux-Roses, etched (50°C, 45 min), and copied at Kodak. T-K-R: radiographed at Pontenay-aux-Roses, etched at Kodak (50°C, 45 min) and copied at Rise. 8 MIN: 8 min exposure to neutrons. 16 MIN: 16 min exposure to neutrons. CN: CN85B film viewed directly. PF: CN85B film viewed through polarizing filters. KL: copy of CN85B on Kodalith film. KT: copy of CN85B on Kodatone film. KB: copy of CN85B on Kodabrom paper.

		R - R		R - R	
		OM	1M	OM	1M
Quality	5		x		
	4	x	x		x
	3	x	x	x	x
	2	x	x	x	x
	1	x	x	x	x

		T - T			T - T			
		GD			DY			
		T	M	R	D4	T	M	R
Quality	5		x	x				
	4	x	x	x		x		
	3	x	x	x		x	x	x
	2	x	x	x	x	x	x	x
	1	x	x	x	x	x	x	x

Fig. 3. Image quality of KBS-3 neutron radiographs on silver halide films

R-R: radiographed and processed at Risø. GD+SR: gadolinium direct technique with SR film. D4+DY: dysprosium transfer technique with D4 film. OM: radiographed with L/d=110. 1M: radiographed with L/d=160. T-T: radiographed and processed at Fontenay-aux-Roses. GD: gadolinium direct technique with T, M, or R film. DY: dysprosium transfer technique with D4, T, M and R film.

### CONCLUSIONS

From the results presented in fig. 2 and 3 the following conclusions can be drawn:

#### Nitrocellulose Film

1) Better collimation ratio (L/d) has usually resulted in improved image quality.

2) The use of the polarizing filters during the assessment of neutron radiographs has scarcely showed any improvement of image quality.

3) The use of Kodatone (positive) instead of Kodalith (negative) film for copying the CN85B film results in improved image quality.

4) Even copies made on Kodabrom paper show radiographs of fair quality.

5) The image quality was rather impaired by using longer exposures to neutrons.

### Silver Halide Film

- 1) A better collimation ratio (L/d) results in radiographs of improved image quality.
- 2) The transfer technique (using Dy converters) yields radiographs of lower quality.
- 3) D4 film produces radiographs of lowest quality for the transfer method.
- 4) Silver halide films used with Gd and the direct exposure technique yield radiographs of higher quality than obtainable from nitrocellulose film and require less exposure to neutrons.

### General Conclusions

On comparing the results obtained with nitrocellulose film with those of silver halide films the following conclusions can be formulated:

- 1) No visible improvement of image quality could be found on comparing the results reached for the CN85B film (and different viewing techniques) and those for silver halide films using the transfer method (100  $\mu$ m Dy).
- 2) To obtain better results with the CN85B film special viewing techniques are required (use of polarized filters or copying on high-contrast film).
- 3) The use of nitrocellulose film requires a longer exposure to neutrons (on the order of the time necessary to expose a single coated silver halide film with the transfer technique).
- 4) The main advantage of nitrocellulose film is its use in radiographing radioactive objects where the transfer technique is necessary for silver halide films. Good image quality, and ease of irradiation and processing can compensate for the disadvantage of using a more complicated viewing technique.

Finally, it must be stressed that the conclusions formulated above are based on a subjective evaluation of image quality of a specific test object (calibration fuel pin). It will be possible to formulate more comprehensive conclusions on the subject when the Euratom Neutron Radiography Working Group Test Program [3] is completed. In that program not only will the calibration fuel pin be redesigned but also beam purity and sensitivity indicators will be used.

### NEED FOR FURTHER INVESTIGATION

To be able to use all the potential advantages of nitrocellulose film in neutron radiography several problems of its application need further clarification. Unlike silver halide film which has been in use for a relatively long time in industrial radiography (neutron radiography included), nitrocellulose film has been used for that purpose only recently. As its main application lies in the field of neutron radiography of radioactive objects, with its limited number of users, it has not been possible to thoroughly investigate all the technical problems of its application as was the case with silver halide film.

Some problems suitable for further investigation are listed below:



1) Exposure to neutrons and its influence on image quality (is it better to have longer exposure and shorter etching time or vice versa?).

2) Temperature and time of etching, (no positive recommendations exist from film manufacturers).

3) The composition and concentration of the etching bath (e.g., in [8] the use of the KOH instead of NaOH is reported).

4) The use of converter screens: directly coated on nitrocellulose film; or use of separate screens (e.g. Kodak BN1 screen with CN85 film).

5) Use of new types of converter screens (as e.g., reported in [8]).

6) Best technique for evaluating neutron radiographic images on nitrocellulose film (e.g., direct viewing, use of filters, copying on film or paper).

These are only a few problems which need clarification. One can say that the whole problem of image formation and detection on nitrocellulose film needs a thorough scientific investigation.

#### REFERENCES

- [1] DOMANUS J.C., Accuracy of dimension measurements from neutron radiographs of nuclear fuel pins. Risø-M-1860. 26.03.1976 (also as paper 3L8 presented at the Eighth World Conference on Nondestructive Testing, Cannes, 6-11.09.1976.
- [2] DOMANUS J.C., Comparison of image quality of nuclear fuel neutron radiographs taken on silver halide and nitrocellulose film. Risø-M-2170, April 1979 (also as paper 2BDD-1 of the Ninth World Conference on Non-Destructive Testing, Melbourne, 18-23.11.1979).
- [3] DOMANUS J.C., Euratom test program for image quality and accuracy of dimensions. To be presented at the First World Conference on Neutron Radiography, San Diego, 7-10.12.1981.
- [4] DOMANUS J.C., Double beam neutron radiography facility of the Research Establishment Risø. Risø-M-1955, Sept. 1977.
- [5] KNUDSEN P., OLSEN J., Six years experience with the double beam neutron radiography facility at the Risø National Laboratory in Denmark. To be presented at The First World Conference on Neutron Radiography. San Diego, 7-10.12.1981.
- [6] LAPORTE A., Evaluation of 10 years use of industrial neutron radiography devices attached to the central reactor Triton. To be presented at the First World Conference on Neutron Radiography, San Diego, 7-10.12.1981.
- [7] ASTM E545-75. Standard method for determining image quality in thermal neutron radiographic testing.
- [8] BARBALAT R., Utilisation de l'installation de neutronographie sur matériaux radioactifs en service sur le réacteur Isis au CEN/Saclay. Mise en oeuvre et exploitation de la nitrocellulose en neutronographie. CEA. CONF 5736. Mai 1981.

MEASURING SIGNAL-TO-NOISE RATIO OF  
TYPICAL NEUTRON RADIOGRAPHS

P. Gade-Nielsen and J. Olsen  
Risø National Laboratory  
DK-4000 Roskilde, Denmark

ABSTRACT

To improve dimensional measurements of nuclear fuel rods by neutron radiography, we have found it useful to measure the signal-to-noise ratio of the radiographs. The signal and the noise are measured by a digital image processing system. By further evaluation of the method we hope to be able to estimate the influence of noise on dimensional measurements. The paper present a simple signal-transfermodel for the neutron radiography process adopted from X-ray radiography. The paper also present preliminary measurements of the signal-to-noise ratio on different films.

---

INTRODUCTION

The aim of the present paper is to promote the concept of noise in neutron radiography. Noise contains no information about the desired signal, it is unwanted and it limits the possibilities for detecting small contrasts.

However, in order to make an assessment of the accuracies one can achieve by e.g. dimension measurements, it is important to know the signal-to-noise ratio on typical neutron radiographs. We have made some preliminary measurements on different film-screen combinations with a film-viewing system, which digitize the radiograph. It is difficult to make any definite conclusions from these few measurements, but we are convinced that the method will give valuable results, when further results have been obtained at e.g. different densities. The theory of noise is a well established concept for the radiographic process of X-rays. In the following we give a short presentation of these imaging and noise models with the modification that we are using neutrons instead of X-rays to expose the film.

Imaging model

Following Panaitescu [1] the model in Fig. 1 describes the radiographic system as a signal transfer channel.

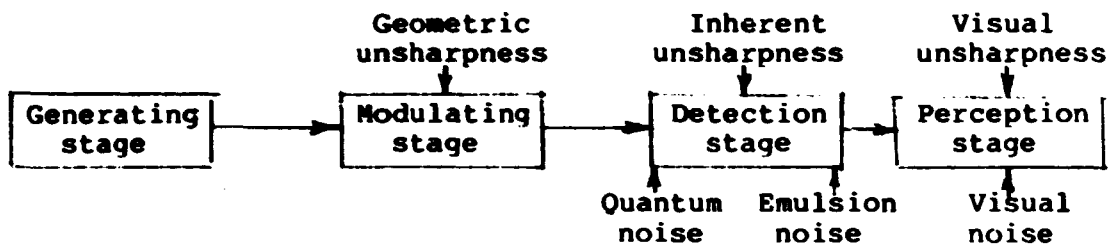


Fig. 1. Model for the neutron radiography process

1. The generating stage is the neutron source.
2. The modulating stage represents the object, which modulates the neutron beam by absorption and scattering.
3. The detection stage is the screen-film combination.
4. The perception stage is the complex operation of detail recognition.

The spatial distortions are observed, when one detects e.g. a sharp edge. It is called the "radiographic unsharpness", and is divided into "the geometric unsharpness" from the modulating stage, "the inherent unsharpness" from the detection stage (screen-film), and "the visual unsharpness" from the perturbation stage. The quantitative measure for the unsharpness effects may be described by either a point spread function (PSF), a line spread function (LSF) or an edge spread function (ESF).

Noise can be described quantitatively by means of its Wiener spectrum, which is derived by Fourier analysis of the random noise pattern. The Wiener spectrum shows the spatial frequency content of the noise.

The white noise is uncorrelated at the input of the detection stage and will be filtered by the point-spread function. In this way one will get a coloured noise (correlated) at the output. The resulting Wiener spectrum is a complicated mixing of quantum noise and film noise.

In the perception stage we get some noise from the electro-mechanical equipment. The noise at the input of the perception stage will be filtered in passing this stage, since all frequencies will not be reproduced correctly. The measured Wiener spectrum will therefore depend upon the perception since the aperture acts as a low-pass filter. The noise is a 2-dimensional stochastic process, and will therefore be fully described by the probability density function in each point, together with the 2-dimensional power-spectrum. Instead of estimating the probability density functions, one often estimates the mean value and the variance, and this will be sufficient if a normal distribution is assumed. By using a larger aperture one averages over several grains, and the central limit theorem leads to a normal distribution regardless of the initial micro distribution.

#### Noise models

To derive an expression for the signal-to-noise ratio, (SNR) the quantitative, structured model as shown in Fig. 2 is used. This simple model can be used to determine the mean value and the variance of the density. It is a static model and the frequency dependent filtering is not taken into account.

White noise:  $E \{ n \} = 0$ ;  $\text{var} \{ n \} = N_A$

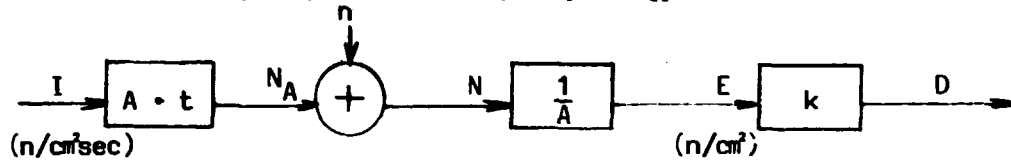


Fig. 2. Model for estimation of the signal-to-noise ratio

The neutrons are poisson-distributed and have the intensity  $I$  over the area  $A$  which one uses in the estimation of  $D$ .  $N_A$  is the expected number of neutrons arriving at  $A$  in the time  $t$ .  $n$  is the uncorrelated fluctuations from the mean value  $N_A$ , and it is assumed that the variance is equal to the mean value  $N_A$ .  $N$  is the total number of neutrons and therefore a stochastic process. The exposure  $E$  is the number of neutrons per unit area in the time  $t$ .  $k$  is the proportionality constant between the exposure and the density, and is assumed to have a constant value for a broad range of exposures.

This is similar to high energetic X-rays [2,3], and the reason is that several grains are affected by every converted neutron.

From the model the expected value of the density is

$$E \{ D \} = k \cdot E = k \cdot I \cdot t \quad (1)$$

and the variance is

$$\begin{aligned} \text{var} \{ D \} &= \text{var} \{ k \cdot E \} = \text{var} \{ k \cdot N/A \} \\ &= (k^2/A^2) \text{var} \{ N \} = (k^2/A^2) \cdot E \{ N \} \\ &= k^2 \cdot I \cdot A \cdot t/A^2 = k^2 \cdot I \cdot t/A \end{aligned} \quad (2)$$

From (2) one gets Selwyn's law:

$$G = A \cdot \text{var} \{ D \} \quad (3)$$

where  $G$  is a constant called the granularity. It means that for a certain exposure  $E$ , the variance of  $D$  will depend upon the chosen area  $A$ .

From equation (2) one can also derive the expression for the variance as given by Siedentopf (1937). To the derivation we will use Nutting's formula [3] as given by the equation.

$$D = \log e \cdot E \{ a \} \cdot N_A/A \quad (4)$$

where  $a$  is the size of the grains (area).

If we introduce  $N_A$ , the number of grains in  $A$ , we find

$$D = \log e \cdot E \{ a \} \cdot E \cdot A \cdot n \cdot m_A/A = k \cdot E \quad (5)$$

where  $n$  is the conversion factor which is equal to the number of neutrons converted, relative to the total number of neutrons, and  $m_A$  is the number of affected grains per converted neutron in  $A$ .

$$k = \log e \cdot E \{ a \} \cdot n \cdot m_A \quad (6)$$

From (2) and (6) we get

$$\text{var} \{ D \} = \log e \cdot D \cdot E \{ a \} \cdot n \cdot m_A / A \quad (7)$$

Siedentopf found the same expression assuming  $n = 1$ , and  $m_A = 1$ , but instead he incorporated the variance of  $a$ . The modified expression for Siedentopf's equation means that the equation can now be given as

$$\text{var} \{ D \} = \log e \cdot D \cdot E \{ a \} \cdot n \cdot m_A / A (1 + \text{var} \{ a \} / E \{ a \}^2) \quad (8)$$

If the signal-to-noise ratio is defined as

$$\text{SNR} = \frac{\text{Expected power in the signal}}{\text{Expected power in the noise}} \quad (9)$$

we get from equations (9), (1), and (2)

$$\text{SNR} = (k \cdot I \cdot t)^2 / (k^2 \cdot I \cdot t / A) = I \cdot A \cdot t \quad (10)$$

If one takes two areas and considers the difference of the densities as the signal, one has

$$\Delta D = D_2 - D_1$$

$$E \{ \Delta D \} = k \cdot t \cdot (I_2 - I_1) \quad (11)$$

$$\text{var} \{ \Delta D \} = k^2 \cdot t (I_1 + I_2) / A \quad (12)$$

$$\text{SNR} = A \cdot t \cdot (I_2 - I_1)^2 / (I_2 + I_1) \quad (13)$$

It is seen from (13) that for a certain radiological contrast  $C = (I_2 - I_1) / (I_2 + I_1)$ , it is only possible to increase SNR by a longer exposure time  $t$ , or by a larger area  $A$ . By increasing  $A$  one will unfortunately also reduce the spatial resolution.

#### Measurement of the noise

The expected value of  $D$  is estimated as the mean value over  $M$  points. The variance of  $D$  is estimated as the mean-square value of the deviations from this mean value.

$$\bar{D} = \frac{1}{M} \sum_{k=1}^M D_k; \quad \sigma_D^2 = \frac{1}{M-1} \sum_{k=1}^M (D_k - \bar{D})^2 \quad (14)$$

When the densities are measured on a radiograph, the value will depend upon the measuring system. The point spread function  $\text{PSP}_M(x,y)$  or its Fourier transformed  $T(u,v)$  is used to characterize the measuring system as illustrated in Fig. 3.

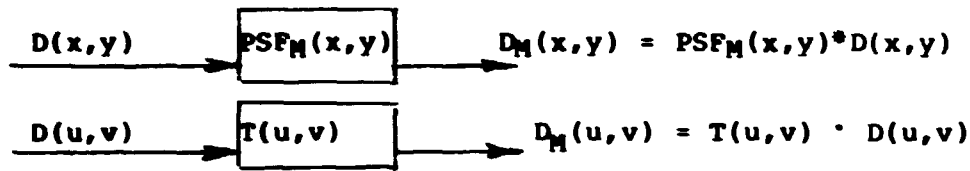


Fig. 3. Transformations of the density in the spatial and the frequency domain.

$D_M$  is the measured density, and  $D$  is the density found with an ideal measuring system ( $T(u,v) = 1$ ). It is assumed that the measuring system adds no additional noise to the measurements.

The variance of the density is the expected power in the signal  $\Delta D(x,y) = D(x,y) - \bar{D}$ . This power can be distributed on harmonic signals to give the power spectrum, and this is called the Wiener spectrum of the radiograph. The measured Wiener spectrum is

$$WS_M(u,v) = |T(u,v)|^2 \cdot WS(u,v) \quad (15)$$

where  $(u,v)$  is the 2-dimensional frequencies.

$WS$  is the Wiener spectrum found with an ideal measuring system ( $T(u,v) = 1$ ).

If the power spectrum is integrated over all frequencies, the result is the total expected power (the variance):

$$\text{var} \{ D \} = \iint WS(u,v) du dv$$

If a large aperture  $A$  compared to the grain size is chosen, it is possible to find  $WS(0,0)$  from [3]

$$WS(0,0) = G = A \cdot \text{var} \{ D \}, \quad (16)$$

where  $G$  is the granularity (3).

Instead of estimating a 2-dimensional Wiener spectrum, it is common practice to estimate 1-dimensional power spectra. If one chooses a certain direction in the 2-dimensional frequency plane as shown in Fig. 4

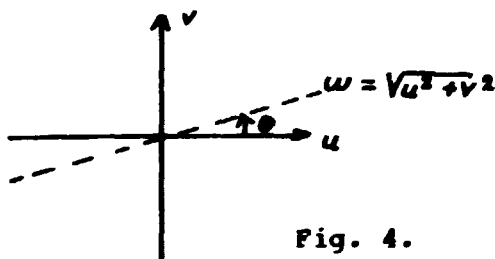


Fig. 4.

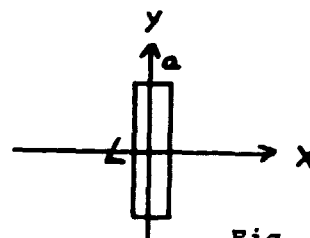


Fig. 5.

one achieves a "section" of the 2-dimensional Wiener spectrum, e.g.  $W(u) = W(u,0)$  for  $\theta = 0$ . If we integrate one frequency out, we get "an integral" Wiener spectrum, e.g.  $W(u) = \int W(u,v) dv$ .

If we find sections for  $\theta$  varying from 0 to  $\pi$ , we will obtain all information about the  $W(u,v)$ . If we assume an isotropic spectrum only one direction is necessary. If a rectangular aperture with the length  $L$  and the width  $a$  as shown in Fig. 5 is used to scan in the  $x$ -direction, one has

$$W_M(u) = W(u,0)(\sin c^2(a \cdot u))/L$$

where

$$\sin c(x) = \sin(\pi x)/(\pi x)$$

$$W_M(u) = W(u,0) \text{ if } L \rightarrow \infty \text{ and } a \rightarrow 0.$$

If one, instead of the rectangular aperture, chooses a point aperture and the scan is taken in the x-direction, one gets the integral spectrum.

$$W_M(u) = \int W(u,v)dv$$

When digitizing equipment is used, one gets free to choose the aperture in the software program when one integrates it from several pixels.

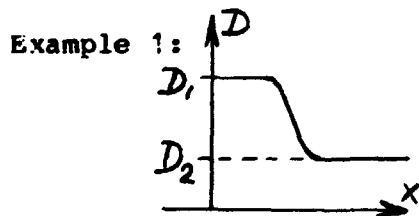
A section of 2-dimensional Wiener spectrum can be estimated from a 1-dimensional sample in the x-direction, when one uses rectangular pixels.

$$WS_M(u) = \frac{1}{M} \left| \sum_{k=1}^M (D_k - \bar{D}) e^{jku} \right|^2 \quad (17)$$

M is the number of samples. There are several other methods to estimate the power spectra [4].

#### The influence of noise on dimensional measurements

In the first example we will use formulas (7) and (16) to estimate the variance of D from the quantum noise and the grain size distribution. The examples chosen are with arbitrary values.



If:  $m_A = 2$

$$a = 5 \mu m^2$$

$$\eta = 0.1$$

$$SNR = (D_1 - D_2)^2 / (\text{var} \{ D_1 \} + \text{var} \{ D_2 \})$$

Fig. 6. Density change

No.	A [ $\mu m^2$ ]	D <sub>1</sub>	D <sub>2</sub>	WS <sub>1</sub> (0) [ $\mu m^2$ ]	WS <sub>2</sub> (0) [ $\mu m^2$ ]	var(D <sub>1</sub> )	var(D <sub>2</sub> )	SNR
1	40	2.0	1.8	0.87	0.78	0.022	0.020	0.95
2	40	2.0	1.0	0.87	0.43	0.022	0.011	31
3	40	4.0	2.0	1.74	0.87	0.044	0.022	62

In case 1 the SNR is too low to make a definite determination of the position. SNR can be increased using a larger aperture A, but this again will make the position more uncertain. From 2 and 3 we see that by doubling the exposure time, we also double the SNR.

Example 2:

A gap in an uranium rod is indicated by a density variation as shown in Fig. 7.

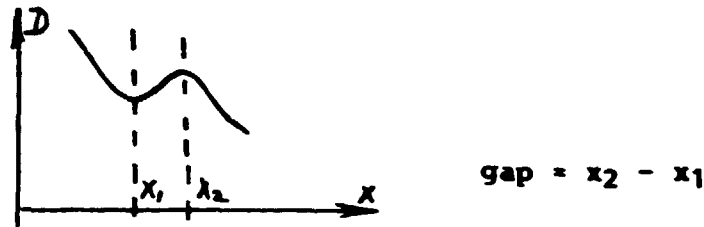


Fig. 7. Density variations for the gap in an uranium rod.

Are we able to detect the gap with an accuracy of 20  $\mu\text{m}$ ? We divide the distance  $x$  in pieces of 10  $\mu\text{m}$ . The question is, do we have a SNR in steps of 10  $\mu\text{m}$  which are high enough to detect a  $\Delta D$  in the curve so that we can determine  $x_2 - x_1$ . The problem is more difficult when we have a smooth curve instead of a jump. It will be convenient to use an aperture with the dimension  $L$  times 10  $\mu\text{m}$  where  $L$  is as large as possible. We assume a normal distributed noise, when we use the area  $A$  to measure the density.

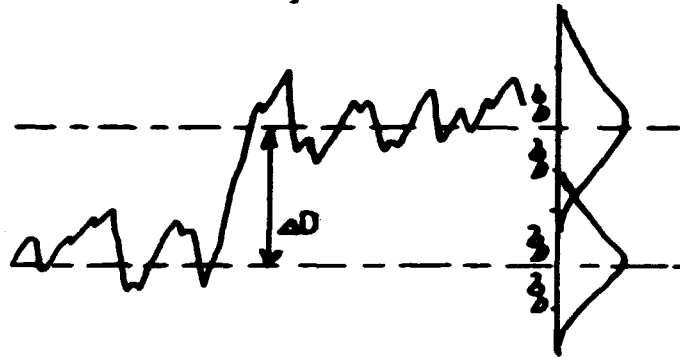


Fig. 8. Density change where the signal is superimposed with noise.

The area  $A$  should be chosen so that the probability of getting density fluctuations greater than  $\Delta D$  is small. This probability is given by

$$p(\sigma_D, \Delta D) = 1 - \frac{1}{\sigma_D \sqrt{2\pi}} \int_{-\Delta D}^{\Delta D} e^{-t^2/(2\sigma_D^2)} dt$$

$$= \text{erfc} \left\{ \Delta D / (\sigma_D \cdot \sqrt{2}) \right\}$$

where  $\sigma_D$  is the standard deviation of the noise.

If  $\Delta D = 2 \sigma_D$ , we get  $p = 4.6\%$ , which means that we in 4.6% of the measurements will get a signal smaller than the noise.  $\Delta D = 3 \sigma_D$  gives  $p = 0.3\%$ .

If we want to detect a signal  $\Delta D = 0.01$  with  $p = 0.3\%$  and  $WS(o) = 10 \mu\text{m}^2$ , we must use  $A = 0.9 \text{ mm}^2$ . With a slit width  $a = 10 \mu\text{m}$ , this results in length  $L = 9 \text{ cm}$ . This seems to be unrealistic. From this one can see that it is important to know the noise before making an assessment of the possibilities of obtaining measurement with a certain accuracy. If one has measured a density curve with sufficient accuracy, the next problem would be to identify edges from the curves, and here some knowledge of the ESF can help.



### Results from the measurements

With a TV-camera and a digitizer we have measured 10 different films with a pixel of  $10 \mu\text{m} \times 13.3 \mu\text{m}$ ,  $A = 133 \mu\text{m}^2$ . To reduce the electric noise 64 digitized images of the same radiograph were added together. The preliminary measurements gave the following results:

No.	FILM	SCREEN	DENSITY	SNR	$W(o)$ [ $\mu\text{m}^2$ ]
1	SR	Gd	1.4	250	1.0
2	D4	Dy	1.6	550	0.6
3	M	Gd	1.8	480	0.9
4	R	Gd	1.7	330	1.1
5	T	Gd	1.7	240	1.6
6	M	Dy	2.0	800	0.7
7	R	Dy	1.9	540	0.9
8	T	Dy	1.1	77	1.9
9	D4	Dy	1.3	250	1.0
10	CN	attached	0.15	19	0.15

More details about the measuring system and the measurements are described in [5]. Unfortunately we have only performed few measurements, but from the results it emerged that a higher density gives a better signal-to-noise ratio.

### Future work

The work with neutron radiography will probably change drastically in the near future when film-viewing systems will be common and so it will be possible to digitize radiographs with a very high resolution. Image processing methods will probably also become common, and it will become easy to estimate the noise and make e.g. dimensional measurements by fitting procedures.

### REFERENCES

- [1] PANAITESCU, I., "Performance Evaluation of Radiographic Systems and Techniques" from "Research Techniques in Non-Destructive Testing", vol. III chapter 8.
- [2] THUESEN, G., Radiography. The Technical University of Denmark, April 1980. (Danish version).
- [3] DAINY & SHAW, Image Science, Academic Press, 1974.
- [4] OPPENHEIM & SCHAFER, Digital Signal Processing, Prentice Hall 1975.
- [5] DEMANDT, K., DOMANUS, J., and GADE-NIELSEN, P., The Measuring of Noise on Neutron Radiographs. Risø 1981. (Presented at the NRWG-meeting in Grenoble, 1980).

Rise - M - 2320

<p>Title and author(s)</p> <p>Neutron radiography at the Rise National Laboratory</p> <p>J.C. Domanus, P. Gade-Nielsen, P. Knudsen, and J. Olsen</p>	<p>Date November 1981</p> <p>Department or group Metallurgy and Reactor Technology</p> <p>Group's own registration number (s)</p>
<p>pages + tables + illustrations</p>	
<p>Abstract</p> <p>In this report six papers are collected which will be presented at the First World Conference on Neutron Radiography in San Diego, U.S.A., 7 - 10-12.1981.</p> <p>They are preceded by a short description of the activities of Rise National Laboratory in the field of post-irradiation examination of nuclear fuel.</p> <p>One of the nondestructive methods used for this examination is neutron radiography.</p> <p>In the six conference papers different aspects of neutron radiography performed at Rise are presented.</p> <p>Available on request from Rise Library, Rise National Laboratory (Rise Bibliotek) Forsøgsanlæg Rise), DK-4000 Roskilde, Denmark Telephone: (02) 37 12 12, ext. 2262. Telex: 43116</p>	<p>Copies to</p>